Received: 19 February 2020 | Revised: 4 June 2020 | Accepted: 5 June 2020

DOI: 10.1111/bre.12484

ORIGINAL ARTICLE

Basin Research | IAS EAGE | WILEY

Supradetachment to rift basin transition recorded in continental to marine deposition; Paleogene Bandar Jissah Basin, NE Oman

Christopher Sæbø Serck[1] | **Alvar Braathen**[1] | **Snorre Olaussen**[2] | **Per Terje Osmundsen**[3] | **Ivar Midtkandal**[1] | **Anna Elisabeth van Yperen**[1] | **Kjetil Indrevær**[1,4]

[1]Department of Geosciences, University of Oslo, Oslo, Norway

[2]Department of Arctic Geology, UNIS, Longyearbyen, Norway

[3]Department of Geoscience and Petroleum, NTNU, Trondheim, Norway

[4]The Norwegian Water Resources and Energy Directorate, NVE, Hamar, Norway

Correspondence
Christopher Sæbø Serck, Department of Geosciences, University of Oslo, P.O. Box 1047, Blindern, 0316 Oslo, Norway.
Email: c.s.serck@geo.uio.no

Funding information
Research Council of Norway, Grant/Award Number: 295208 and 228107

Abstract

A transition from supradetachment to rift basin signature is recorded in the ~1,500 m thick succession of continental to shallow marine conglomerates, mixed carbonate-siliciclastic shallow marine sediments and carbonate ramp deposits preserved in the Bandar Jissah Basin, located southeast of Muscat in the Sultanate of Oman. During deposition, isostatically-driven uplift rotated the underlying Banurama Detachment and basin fill ~45° before both were cut by the steep Wadi Kabir Fault as the basin progressed to a rift-style bathymetry that controlled sedimentary facies belts and growth packages. The upper Paleocene to lower Eocene Jafnayn Formation was deposited in a supradetachment basin controlled by the Banurama Detachment. Alluvial fan conglomerates sourced from the Semail Ophiolite and the Saih Hatat window overlie the ophiolitic substrate and display sedimentary transport directions parallel to tectonic transport in the Banurama Detachment. The continental strata grade into braidplain, mouth bar, shoreface and carbonate ramp deposits. Subsequent detachment-related folding of the basin during deposition of the Eocene Rusayl and lower Seeb formations marks the early transition towards a rift-style basin setting. The folding, which caused drainage diversion and is affiliated with sedimentary growth packages, coincided with uplift-isostasy as the Banurama Detachment was abandoned and the steeper Marina, Yiti Beach and Wadi Kabir faults were activated. The upper Seeb Formation records the late transition to rift-style basin phase, with fault-controlled sedimentary growth packages and facies distributions. A predominance of carbonates over siliciclastic sediments resulted from increasing near-fault accommodation, complemented by reduced sedimentary input from upland catchments. Hence, facies distributions in the Bandar Jissah Basin reflect the progression from detachment to rift-style tectonics, adding to the understanding of post-orogenic extensional basin systems.

The peer review history for this article is available at https://publons.com/publon/10.1111/bre.12484.

KEYWORDS
carbonates, extensional tectonics, rift basins, supradetachment basin

1 | INTRODUCTION

Extensional basin analysis comprises descriptions of dip and displacement on their bounding faults, stretching factors, subsidence/uplift rates, drainage style and sedimentary architecture, compliant with either rift- or supradetachment basin styles (Friedmann & Burbank, 1995). Supradetachment systems are characterized by significantly higher crustal extension rates than rift systems (Friedmann & Burbank, 1995). Rift basins (e.g. Gawthorpe, Fraser, & Collier, 1994; Gupta, Cowie, Dawers, & Underhill, 1998; Henstra, Gawthorpe, Helland-Hansen, Ravnås, & Rotevatn, 2017; Rattey & Hayward, 1993; Ravnås & Steel, 1998) and supradetachment basins are well-covered in literature, with cases of the latter found for e.g. the North Atlantic margin (Osmundsen & Péron-Pinvidic, 2018), the Italian Dolomites (Massari & Neri, 1997), the Scandinavian Caledonides (e.g. Braathen, Osmundsen, Nordgulen, Roberts, & Meyer, 2002; Osmundsen & Andersen, 2001; Osmundsen, Bakke, Svendby, & Andersen, 2000; Vetti & Fossen, 2012), the Aegean (e.g. Asti et al., 2019; Asti, Malusà, & Faccenna, 2018; van Hinsbergen & Meulenkamp, 2006; Oner & Dilek, 2011), Tibet (Kapp, Taylor, Stockli, & Ding, 2008) and pre-Basin and Range western U.S. (e.g Fillmore, Walker, Bartley, & Glazner, 1994; Friedmann & Burbank, 1995). Recent consensus advocates that successive generations of linked faults and detachments result in spatio-temporal domains with distinct geometries, challenging simplistic classifications of rift- and supradetachment basins (e.g. Braathen & Osmundsen, 2020; Brun et al., 2018; Manatschal, 2004; Osmundsen & Péron-Pinvidic, 2018; Sutra, Manatschal, Mohn, & Unternehr, 2013). For instance, supradetachment basins may be truncated by steep rift-style faults above new, deeper detachments as higher-level detachments are abandoned during uplift and rotation (Figure 1; Asti et al., 2019; Fedo & Miller, 1992; Friedmann & Burbank, 1995). Following this line of attack, our investigation of the basin fill in the Paleogene Bandar Jissah Basin in northeastern Oman highlights sedimentary response to interlinked detachment and fault activity.

Rift faults exert local geomorphological control while the large-magnitude extensional detachments associated with supradetachment basin systems accommodate major crustal thinning that trigger isostatic uplift of broad regions, modifying the orientation of structures and basins (Asti et al., 2019; Friedmann & Burbank, 1995; Gawthorpe & Leeder, 2000; Oner & Dilek, 2011; Schlische, 1995; Stein & Barrientos, 1985). Effects of major isostatic adjustments are broadly debated to explain nearly horizontal major shear zones, exhumed from the middle crust, with their exhumation process leading to significant rotation, as advocated in rolling-hinge models (Brun et al., 2018; Lister & Davis, 1989). Different supradetachment basin types can co-exist in the same supradetachment system because of dip variations (ramp-flat-ramp) in the underlying, controlling detachment (Asti et al., 2019; Vetti & Fossen, 2012). Furthermore, folds are inherent features of any extensional basin, where variations in the controlling faults give rise to both fault-parallel and fault-perpendicular folds that may influence the geomorphology, and thus the depositional systems (e.g. Friedmann & Burbank, 1995; Gawthorpe & Leeder, 2000; Kapp et al., 2008; Schlische, 1995; Serck & Braathen, 2019).

On a different note, broad isostatic uplift from detachment movements produce large sediment source areas and basin fill dominated by alluvial fan deposits resulting from extension-parallel (detachment-transverse) transport of sediments derived from within the basin system (Friedmann & Burbank, 1995; Oner & Dilek, 2011). Basin fill in many cases record a transgressive development from alluvial fans via braided streams to fan deltas and carbonate ramps (Massari & Neri, 1997), reflecting a setting of mixed shallow marine carbonate-siliciclastic depositional systems that may prevail in low-latitude areas with arid climatic conditions and elevated drainage catchments (e.g. rift shoulders or pre-rift orogens). The arid conditions favour ephemeral runoff from hinterland catchments, leading to deposition of continental to marginal marine coarse clastic sediments. Down depositional dip, the coarse clastic sediments grade into marine carbonates produced under favourable conditions, as highlighted in this study. Examples include the Miocene deposits of the Lorca Basin, Spain (Thrana & Talbot, 2006), the Miocene Suez Rift strata with recent analogues (Cross & Bosence, 2008; Cross, Purser, & Bosence, 1998; Friedman, 1988; Roberts & Murray, 1988), Upper Jurassic sediments in the Neuquén Basin (Spalletti, Franzese, Matheos, & Schwarz, 2000),

Highlights

- The Bandar Jissah Basin in Oman evolved from a supradetachment basin to a rift basin system.
- Lower basin fill dominated by high-energy continental deposits controlled by the Banurama detachment.
- Younger faults dissected the upper-plate rocks, cutting the rotated detachment and basin fill.
- Carbonate-dominated upper basin fill controlled by steep rift-style faulting.

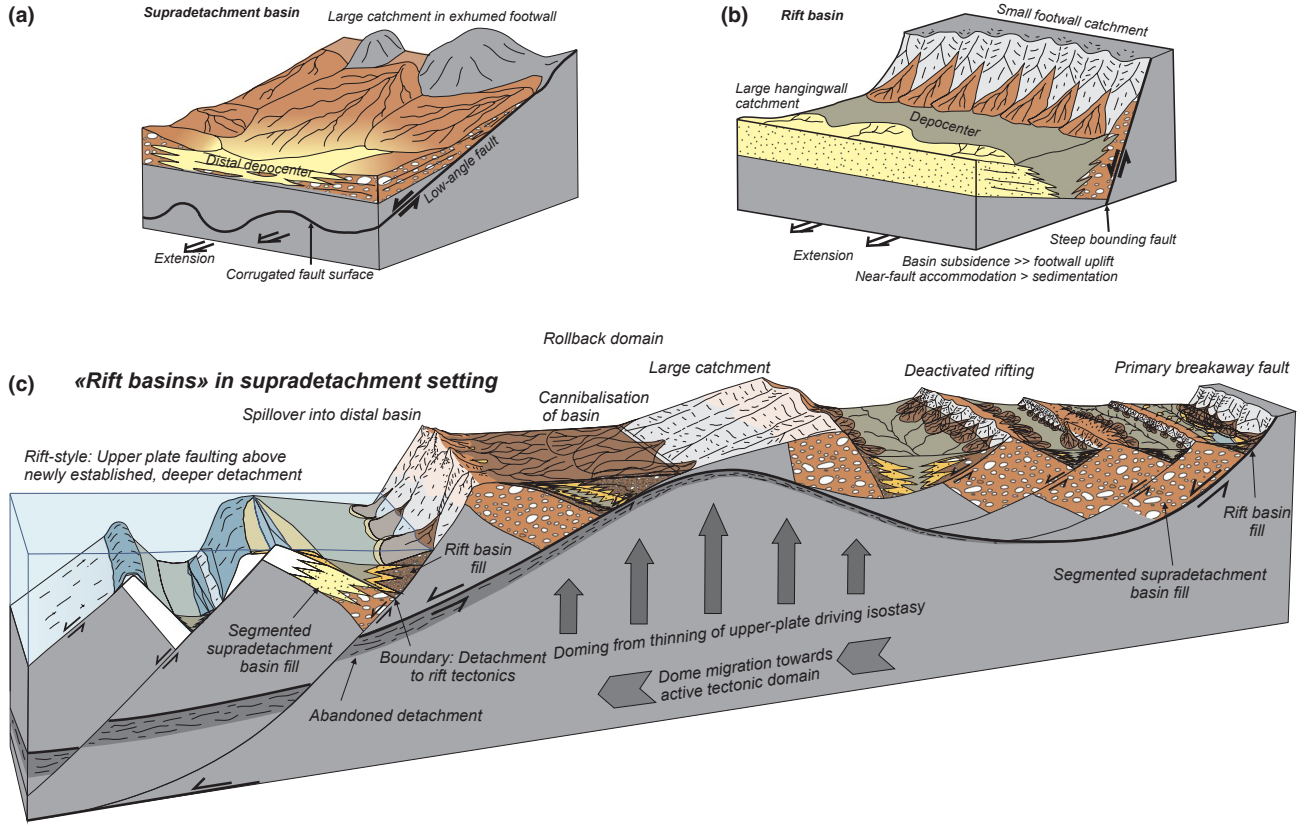

FIGURE 1 Extensional basin types and combined tectonic setting. (a) Rift basin, (b) supradetachment basin and (c) rift-style basins in a supradetachment setting. (a) and (b) redrawn and modified after (Friedmann & Burbank, 1995)

the Carboniferous succession in the Billefjorden Trough on Svalbard (Braathen, Bælum, Maher, & Buckley, 2011; Smyrak-Sikora, Johannessen, Olaussen, Sandal, & Braathen, 2019) and Devonian deposits in the Canning Basin, Western Australia (Holmes & Christie-Blick, 1993).

This article is devoted to basin characteristics during the transition between different extensional basin styles. We demonstrate how sedimentation in the Paleogene Bandar Jissah Basin changed as the controlling mode of deformation evolved from detachment to high-angle extensional faulting (Figures 2 and 3). Our investigation shows that the early detachment-style basin fill was dominantly transgressive, with depositional environments spanning from alluvial fans to carbonate ramps. The transition to a rift-style basin system was recorded by mixed carbonate-siliclastic shallow marine deposits that occasionally experienced subaerial exposure. Eventually, the basin became truly carbonate-dominated as sediment sources in the footwall were cut-off or became exhausted.

2 | GEOLOGICAL SETTING

The Oman Mountains (Al-Hajar Mountains) features the world's most well-studied ophiolite complex (e.g. Rollinson, Searle, Abbasi, Al-Lazki, & Al Kindi, 2014). Inside the range, the Semail Ophiolite forms part of a nappe stack of Permian to Upper Cretaceous shelf- to deep-water rocks that was obducted onto the Arabian Neo-Tethys margin during the Late Cretaceous (e.g Cooper, Ali, & Searle, 2014; Glennie et al., 1973; Glennie et al., 1974; Lippard, Shelton, & Gass, 1986; Searle, 2007; Searle, Warren, Waters, & Parrish, 2004). Subsequent extensional collapse of this orogen is evidenced by the Jebel Akhdar and Saih Hatat tectonic windows. Eclogite facies rocks that were exhumed from depths exceeding 30 km in the Late Cretaceous currently outcrop in the Saih Hatat window/metamorphic core complex (Figure 2a; e.g. Lippard, 1983). Sediments were shed to surrounding areas and alluvial fan conglomerates of the Al Khawd and Qahlah formations developed directly on the Semail Ophiolite northeast of the orogen in the Late Campanian-Maastrichtian (Mann, Hanna, & Nolan, 1990; Nolan, Skelton, Clissold, & Smewing, 1990). Exhumation of Saih Hatat is recorded by the reverse stratigraphy of Al Khawd and Qahlah Formation conglomerates, where clasts derived from structurally highest nappes were deposited lowest in the post-obduction stratigraphy (Abbasi, Salad Hersi, & Al-Harthy, 2014; Nolan et al., 1990). Several periods of extension have been suggested to have followed ophiolite obduction based on field data from Upper Cretaceous to

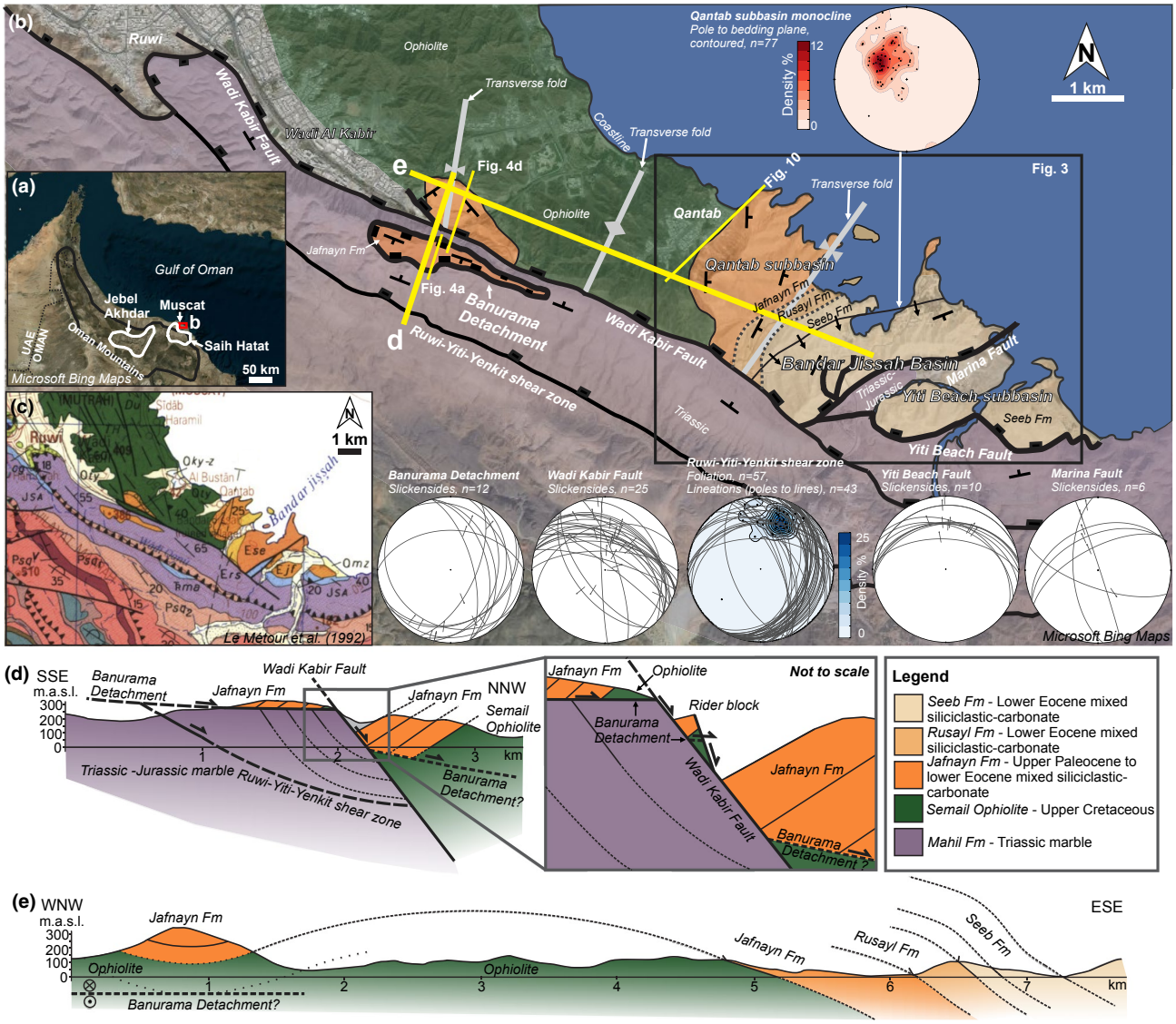

FIGURE 2 (a) Overview map showing the NE Arabian Peninsula. Red box gives location of (b). (b) Main structural elements of the larger study area between Ruwi and Yiti Beach modified from Le Métour et al. (1992). Stereoplots for the Wadi Kabir, Marina and Yiti Beach faults display fault planes and slickenlines. Banurama Detachment stereoplot shows fault planes with slickenlines. Ruwi-Yiti-Yenkit shear zone stereoplot displays foliations and lineations (contoured poles to lines). Stereoplot for the Qantab subbasin monocline displays contoured poles to bedding planes. Satellite photo courtesy of Bing/Microsoft. (c) Geological map of the study area by Le Métour et al. (1992), included for comparison with our interpretations. Abbreviations of Paleogene formations: E_{jf} – Jafnayn Formation, E_{rs} – Rusayl Formation, E_{se} – Seeb Formation. (d) Cross-section perpendicular to the Wadi Kabir Fault showing the structural relationship between the Banurama Detachment and Wadi Kabir Fault. Cross-section location shown in (b). Inset emphasize rider block with outcropping Banurama Detachment on Wadi Kabir Fault. (e) Wadi Kabir fault-parallel hanging wall cross-section displaying relation between Paleogene deposits in the Wadi al Kabir and Qantab areas

lower Eocene sedimentary growth packages and interpretation of steep faults in post-obduction slope sediments offshore northern Oman (Fournier, Lepvrier, Razin, & Jolivet, 2006; Mann et al., 1990; Mattern & Scharf, 2018; Ricateau & Riche, 1980; White & Ross, 1979). Extensional faulting controlled post-obduction deposition and led to rapid lateral thickness and facies variations in Upper Cretaceous to Eocene strata (Abbasi et al., 2014; Mann et al., 1990; Nolan et al., 1990). Fournier et al. (2006) suggested that extensional faulting persisted until the early Eocene, when deposition of the Jafnayn Formation was affected by syn-sedimentary normal faults. A major regional unconformity separates Upper Cretaceous from Paleocene strata. Paleocene to lower Eocene strata (Jafnayn and Rusayl formations) thin and onlap towards Saih Hatat, indicating its topographic prominence and role as a sediment source area (Searle, 2007). However, presence of Seeb Formation open-shelf limestones with little/insignificant terrigenous input in and around the Oman Mountains suggests that the Saih Hatat was submerged by the middle Eocene (Hansman, Ring, Thomson, den Brok, &

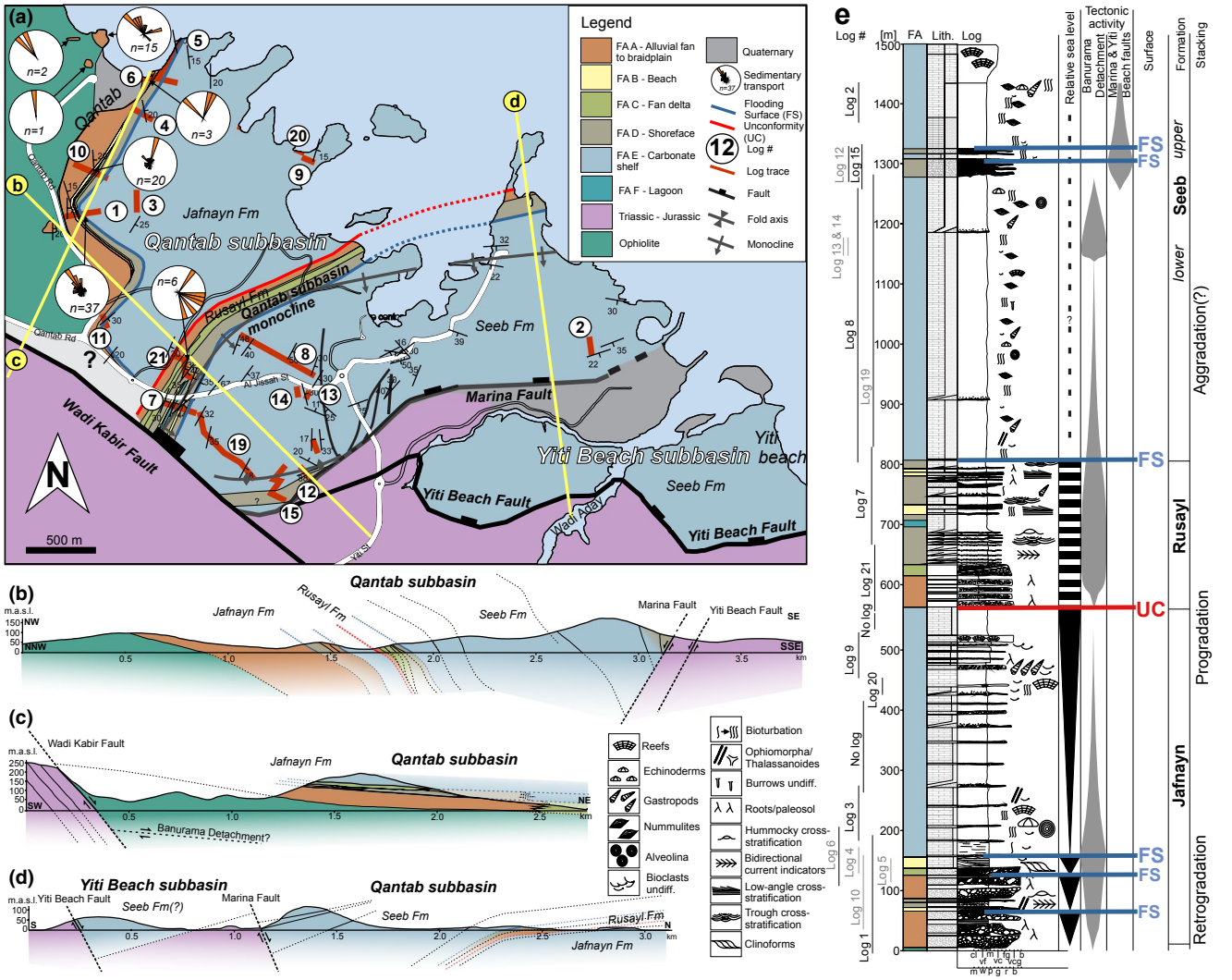

FIGURE 3 (a) Mapped facies associations in the Bandar Jissah Basin with structural measurements, log traces reported in Figure 5 and paleocurrent measurements. Main structural elements annotated. Location shown in Figure 2b. Modified after Le Métour et al. (1992). (b, c and d) show cross-sections with key structural and stratigraphic features. Profile locations in (a). (e) Displays a composite log through the Bandar Jissah Basin succession

Stübner, 2017; Nolan et al., 1990). Hence, uplift of the Al Hajar Mountains to their current elevation (highest peak is Jebel Shams, 3,000 m.a.s.l.) took place during or after the late Eocene. The timing and cause for the uplift is debated; Miocene (Saddiqi, Michard, Goffe, Poupeau, & Oberhänsli, 2006), Oligocene (Gray, Kohn, Gregory, & Raza, 2006; Mount, Crawford, & Bergman, 1998; Würsten et al., 1991) or late Eocene to middle Miocene (Hansman et al., 2017) uplift have been suggested. Suggested causes for the uplift include far-field stresses from the Zagros collision (Ali & Watts, 2009; Fournier et al., 2006; Glennie et al., 1974; Nolan et al., 1990; Searle & Ali, 2009) or crustal thickening following a retardation of Makran subduction causing north Oman to accommodate Arabia-Eurasia convergence (Hansman et al., 2017). A complementary view is that post-obduction extension of the Semail Ophiolite lasted throughout the Eocene (Braathen & Osmundsen, 2020). Another phase of extension that started in the Oligocene has been suggested by Fournier et al. (2006). The following brief review based in literature is complicated by the tectonic picture; growth basins around the Saih Hatat culmination may differ significantly in terms of sedimentary facies distributions although they are the results of the same tectonic event(s). This hampers regional stratigraphic correlations.

The Paleocene to Eocene sedimentary succession in northeastern Oman consists of the Jafnayn, Rusayl and Seeb formations. They are all dominated by carbonates formed in a shallow marine environment, but they vary in terms of depositional subenvironments, fossil fauna and siliciclastic content (Figure 3). The characteristics of the late Paleocene Jafnayn Formation vary between localities in terms of thickness, amount of terrigenous debris and substrate. In the Bandar Jissah Basin, Jafnayn Formation conglomerates are deposited directly onto the Semail Ophiolite

(Fournier et al., 2006; Le Métour, Béchennec, Roger, & Wyns, 1992; Mann et al., 1990; Nolan et al., 1990; Özcan et al., 2016; Racey, 1995). The Jafnayn Formation records a regional transgression event during the late Paleocene and consists primarily of shallow-shelf wackestones to grainstones. Larger benthic foraminifera such as *Orbitolites*, miliolids and *Alveolina*, together with coral fragments, mixed carbonate-siliciclastic sandstones and conglomerate interbeds, reflect variable energy and water depth on the shelf (Haynes, Racey, & Whittaker, 2010; Nolan et al., 1990; Özcan et al., 2016; Racey, 1995).

The Rusayl Formation consists of varied deposits that record an early Eocene regression. Sediments grade from shales and marls with miliolids, storm beds and oyster rudstones to crossbedded sandstones, representing depositional environments that range from lagoons or mangrove swamps to high-energy storm-influenced barrier complexes (Beavington-Penney, Wright, & Racey, 2006; Dill et al., 2007; Nolan et al., 1990; Özcan et al., 2016; Racey, 1995).

The Seeb Formation consists of nodular foraminiferal wackestones to grainstones with a varied fossil assemblage that indicate energy variations in a carbonate ramp setting with an overall transgressive trend (Beavington-Penney et al., 2006; Nolan et al., 1990; Racey, 1995). In the lower part of the Seeb Formation the microfauna is dominated by *Alveolina* and miliolids, while the upper part display a predominance of *Nummulites* and *Assilina* at the type locality (Nolan et al., 1990). Bio-retexturing is generally complete although occasional storm beds and preserved hummocky cross-stratification suggest the carbonate ramp was wave-affected (Beavington-Penney et al., 2006). Some karstification and paleosol development in the Seeb Formation reflect intermittent subaerial exposure (Dill et al., 2007).

The study area is located between Yiti Beach and Wadi Al Kabir, SE of Muscat in the Sultanate of Oman (Figure 2). The area was mapped by Le Métour et al. (1992) (Figure 2c) and included in studies by Racey (1995), Searle et al. (2004), Fournier et al. (2006) and Haynes et al. (2010).

In its current configuration, the southern margin of the Bandar Jissah Basin is bounded by three faults: The NW striking Wadi Kabir Fault, the Marina Fault striking WSW, and the Yiti Beach Fault striking approximately W (Figures 2b and 3a). Paleocene to Eocene strata are preserved in the hanging walls of these faults. Towards the northwest, the footwall of the Wadi Kabir Fault contains an outlier klippe of moderately SW-dipping Paleogene strata (Figure 2). This klippe is bound underneath by the sub-horizontal Banurama Detachment, which separates it from underlying north-dipping Triassic low-grade metamorphic carbonates, henceforth termed marbles for simplicity (Figure 4a; Braathen & Osmundsen, 2020). In the northernmost part of the outlier, Eocene strata rests unconformably on the ophiolite over the Banurama Detachment. The Wadi Kabir Fault truncates and offsets this detachment down to the NE (Figure 4d). Hence, the Bandar Jissah Basin with its depositional substrate sits in an allochthonous position, which is cut and offset by the younger and steeper Wadi Kabir Fault. Together with the Marina and Yiti Beach faults, the Wadi Kabir Fault represents faulting that post-date the Banurama Detachment. The basin fill consequently records two different settings: An initial basin setting controlled by the detachment and a later setting controlled by the steeper faults.

We subdivide the Bandar Jissah Basin into the informally named Qantab and Yiti Beach subbasins. The former is located NW of the Marina Fault towards Muscat and the latter occupies a position between the Marina and Yiti Beach faults (Figures 2 and 3). Qantab subbasin strata onlap ophiolitic rocks above a 5–10 m high paleo-relief. Footwall rocks to the south consists of Triassic to Jurassic low-grade carbonates (marbles).

Contractional inversion has been proposed for the basin (Fournier et al., 2006). However, we observe mostly extensional structures and see no evidence for syn-contractional deposition. Accordingly, we will not discuss contraction or inversion structures in this work.

3 | METHODS

Conventional fieldwork was carried out over a period of four weeks in January and December 2017, measuring sedimentological sections and collecting structural data (Figures 2, 3 and 5). The dataset includes a large collection of photographs including high-resolution photomosaics suitable for analysis of depositional architecture of km-scale outcrops. Structural measurements were plotted using OpenStereo software (Grohmann & Campanha, 2010). The basin stratigraphy is divided into facies based on depositional processes (Table 1). Carbonate-dominated facies are classified according to Dunham (1962) and Embry and Klovan (1971). Facies associations define depositional environments (Figures 6 and 7). 25 thin sections were made from collected rock samples to determine their ages and depositional sub-environments (Figure 8).

4 | RESULTS AND INTERPRETATION

4.1 | Facies associations

4.1.1 | FA A

Description

FA A consists predominantly of gravel to boulder conglomerates with sandy and silty interbeds (Facies 1, 2, (3), 4.1,

4.2, 7; Table 1; Figures 6 and 7a). Conglomerate beds display normal, inverse, normal-to-inverse or no grading. Bases of conglomerate beds vary from strongly erosive (typical for normal graded beds) to non-erosive (typical for inverse graded or ungraded beds). Clast sorting and internal organization/clast fabric of individual conglomerate beds range from unsorted and disorganized to better sorting with well-developed clast fabrics, the latter more typical for normal-graded conglomerate beds and with a higher occurrence frequency towards northeast. Similarly, silty sandstone (Facies 7) deposits that drape conglomerate beds and fill scour/channel features are increasingly preserved towards the northeastern part of the study area.

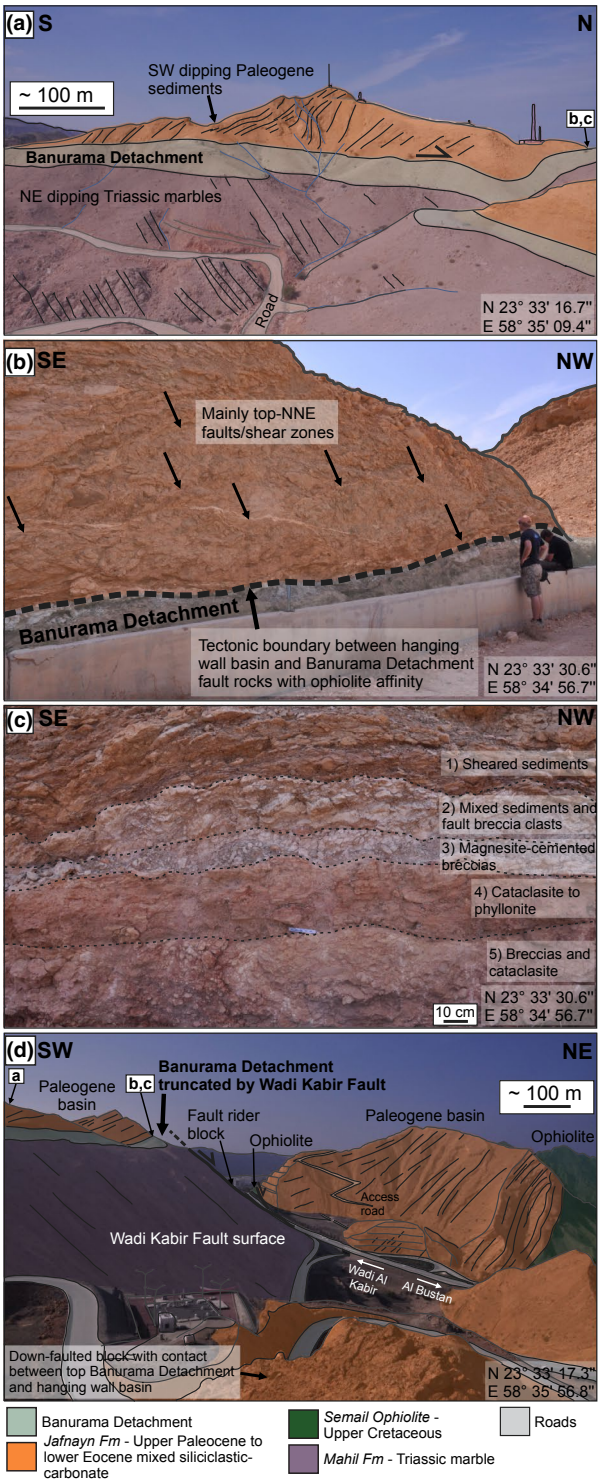

FIGURE 4 The Banurama Detachment and relationship with the Bandar Jissah Basin. The approximate extents of the photos are shown in Figure 2. (a) The 10–30 m thick Banurama Detachment separates NE dipping Triassic marbles from SW dipping Paleogene sediments (Jafnayn Formation). Tectonic transport in the Banurama Detachment is top-to-NNE. (b) The boundary between the Banurama Detachment and the Paleogene basin in its hanging wall. See (a) for location of photo. (c) Details of fault rocks at the boundary between the Banurama Detachment and the Paleogene hanging wall basin. The boundary is constituted by several distinct rock units: 1) Sheared out marls and disintegrated limestone beds in the highly sheared basal part of the sedimentary succession in the proximal hanging wall of the detachment, 2) mixed layer of disintegrated hanging wall sediments and clasts of underlying fault breccias, 3) tectonic breccias of serpentine cataclasites cemented by white magnesite, 4) cataclasite to phyllonite in semi-brittle shear zone partly comprising talc-serpentine fabric, 5) carbonate and serpentine breccias superimposed on serpentine cataclasites with remnant clasts of ultramafic rocks from the ophiolite in the footwall of the detachment. Units 1) and 2) in particular display low-angle down-to-NE shear zones. (d) The Wadi Kabir Fault offsets the Banurama Detachment with its Paleogene hanging wall basin down-to-the-NE approximately 500 m (Braathen & Osmundsen, 2020). Note location of photo (a) and (b) in the footwall of the Wadi Kabir Fault. Modified from Braathen and Osmundsen (2020). A version of this figure without interpretation is included as Supplementary Material

Interpretation

FA A represents a spectrum of alluvial fan to braidplain deposits characterized by high relief and significant discharge events. Flow types range from cohesive mass flows, seen as coarse, disorganized, ungraded or inverse graded beds suggesting steep gradients and high discharge, to fully turbulent streamflow as indicated by strongly erosive, normal graded beds with well-developed internal structure (e.g. Talling, Masson, Sumner, & Malgesini, 2012; Zavala, Arcuri, Di Meglio, Diaz, & Contreras, 2011). These unconfined mass flow conglomerates and scouring braided stream conglomerates represent a proximal alluvial fan depositional setting. Furthermore, very coarse deposits and immature flow types in the sedimentary record suggest proximity to a high-relief source area. The limited thickness and lateral persistence of paleosols (Facies 7) in the proximal alluvial fan relate to (a) frequent blanketing by unconfined debris flows that inhibits soil development and (b) rapid avulsions in braided river systems, eroding into paleosols (Facies 7). The preservation potential of paleosols (Facies 7) increase from proximal alluvial fan to distal alluvial fan and braidplain, where the depositional gradient was lower and flows were more turbulent. Turbulent flows scoured into the substrate and kept channel belts entrenched with

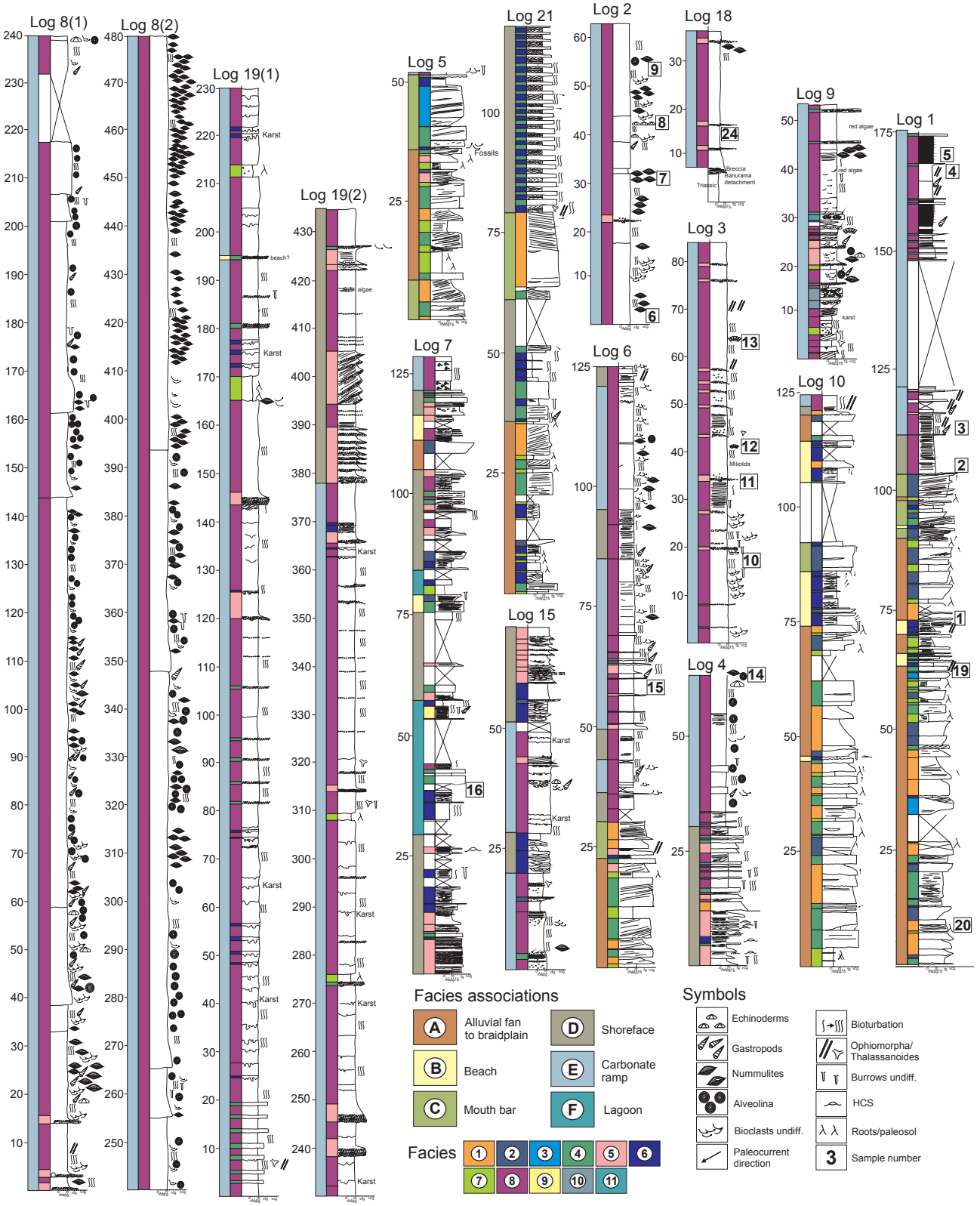

FIGURE 5 Relevant sedimentary logs from the Bandar Jissah Basin and the outlier in the footwall of the Wadi Kabir Fault (log 18). Sample locations annotated. A high-resolution version of this figure is included in Supplementary Material

TABLE 1 Bandar Jissah Basin facies

Facies	Subfacies	Grain size	Description	Depositional process	Remarks	Bed thickness
1. Normal graded conglomerate		vfg-co	Poorly sorted normal graded conglomerate with no stratification or inclined clast fabric and tangential foresets, variably erosive bases, rare sandy clinothems, no visible fossils	Streamflow (erosive bases), debris flow, high-density turbidity current	Variable-depth braided stream deposits where pronounced basal erosion, otherwise waning current debris flows. High-density turbidites where associated with tangential foresets. Sandy clinothems from waning river current or flow separation as flow meets standing water.	<0.5 to >3 m
2. Inverse graded conglomerate		fg-co	Poorly sorted inverse graded conglomerate with rare weak imbrication and horizontal clast fabric. Rare foresets and weakly- or non-erosive bases.	Mass flow	Alluvial fan mass flow deposits with "freeze" deposition. Increasingly organized clast fabric and bedding indicates grading into more fluidal, turbulent flow or waxing current streamflow.	1–5.5 m
3. Inverse-to-normal graded conglomerate		mg-vcg	Well-developed inverse-to-normal graded conglomerate with non-erosive base.	Subaqueous mass flow to high-density turbidity current	Shallow-marine mass flow developing into high-density turbidity current	1.5 m
4. Non-graded conglomerate	4.1. Very poorly sorted	vfg-co	Ungraded and unsorted conglomerate with no or weakly developed bedding, little to no basal erosion and frequent outsized clasts. Occasionally poorly developed clast fabric. Lateral bed pinchout.	Subaerial cohesive mass flow, occasionally increased turbulence	Cohesive mass flow deposits in proximal alluvial fan.	0.2 to ~6 m
	4.2. Foresetted	cg-b	Non-graded, erosively based foresetted conglomerate showing grain size variations across well-defined clinoform surfaces. Individual clinothems show normal grading. Sandy layers.	Fluidal flow	Proximal alluvial fan deposits	<1–2.5 m
	4.3. Carbonate grain matrix	fg-cg	Non-graded, clast-supported siliciclastic conglomerate with carbonate sandstone matrix (facies 8)	High-density turbidity current	Shallow-marine turbidite, likely deposited during periods of increasing run-off in nearby river systems. Likely Facies 5 beds with eroded top.	<0.5 m
	4.4. Very well sorted (log 7)	fg	Non-graded, very well sorted and rounded quartz gravel conglomerate showing parallel bedding and low-angle cross-bedding.	Oscillatory current (waves)	Beach deposit	2 m
5. Graded conglomerate-sandstone		f-co	Normal graded conglomerate to sandstone with slight basal erosion, mixed-lithology sandy matrix showing increasing dominance of carbonate grains up bed. Frequent outsized clasts. Sandstone displays asymmetric ripples, parallel lamination, trough-, sigmoidal-, hummocky- and herringbone cross-stratification. Ophiomorpha burrows. Rare double mud drapings on cross-sets and parallel laminations. Rare conglomeratic foresets.	Tempestites or high-density turbidity current reworked by directional and oscillatory currents	Shallow-marine tempestites or turbidites with reworking of sandy upper part by waves and tidal currents	0.5–3 m (occasionally up to 6 m)

(Continues)

TABLE 1 (Continued)

Facies	Subfacies	Grain size	Description	Depositional process	Remarks	Bed thickness
6. Sandstone		vf-c	Ungraded siliciclastic sandstone with varying content of carbonate grains, body fossils of gastropods and undifferentiated skeletal fragments. *Ophiomorpha* burrows and gravel horizons. Parallel lamination, asymmetrical ripples, low-angle-, tangential-, trough- and hummocky cross-stratification. Scale of cross-sets varies from laminae to m-scale dune cross-stratification. Uni- and bi-directional currents indicated.	Oscillatory (wave) and bidirectional (tidal) current	Lower shoreface to beach environment affected by waves and tides.	~0.2 to 8 m
7. Silty sandstone		si-f	Poorly sorted silty sandstone showing distinct mottling with repeated colour alternations; white, yellow, orange, dark red. Abundant roots and uneven bases, and thus, bed shapes; infills channels, scours and karst topography. Gravel horizons.	Directional current, suspension settling	Paleosols developed in sandy overbank deposits in alluvial fan and braidplain.	cm's–5 m
8. Grainstone to wackestone		f-m	Nodular grainstones to wackestones with variable proportion of siliciclastic grains. Microfauna dominated by *nummulites, alveolina* and other larger benthic foraminifera. Macrofossils include gastropods, echinoids, bivalves/oysters and coral fragments, often dispersed, occasionally in large bank-forming multi- or single-species accumulations. For the most part fully bio-retextured, pockets of preserved sedimentary structure shows parallel laminations, trough- and low-angle cross-stratification. Deposits also display *ophiomorpha* burrowing, gravel horizons and frequent karstification.	Oscillatory(wave) and (bi)directional(tidal) current	Carbonate ramp deposits affected by (storm) wave and tidal currents and bio-retexturing by seagrass roots and burrowing organisms.	m's–10's m's
9. Marl		cl-vf	Extensively bioturbated (*ophiomorpha*) multicoloured (beige to dark red) marl with occasional preserved parallel laminations. Gastropods and skeleteal fragments.	Suspension settling, (bi) directional current	Protected lagoonal environment.	0.5–9 m
10. Rudstone		Rud	Rudstone consisting of highly abraded gastropods, coral fragments, large benthic foraminifera, oyster fragments and undifferentiated thick shell fragments.	Oscillatory current (waves)	Wave-breaking bar.	1–3 m
11. Boundstone		—	Boundstone consisting almost exclusively of corals. Thickness vary from less than 1 m (log 20) to more than 10 m (near Yiti Beach fault)	Biogenic growth	Coral reefs, patchy on carbonate ramp or large buildups on bathymetric highs	0.5–10's of m's

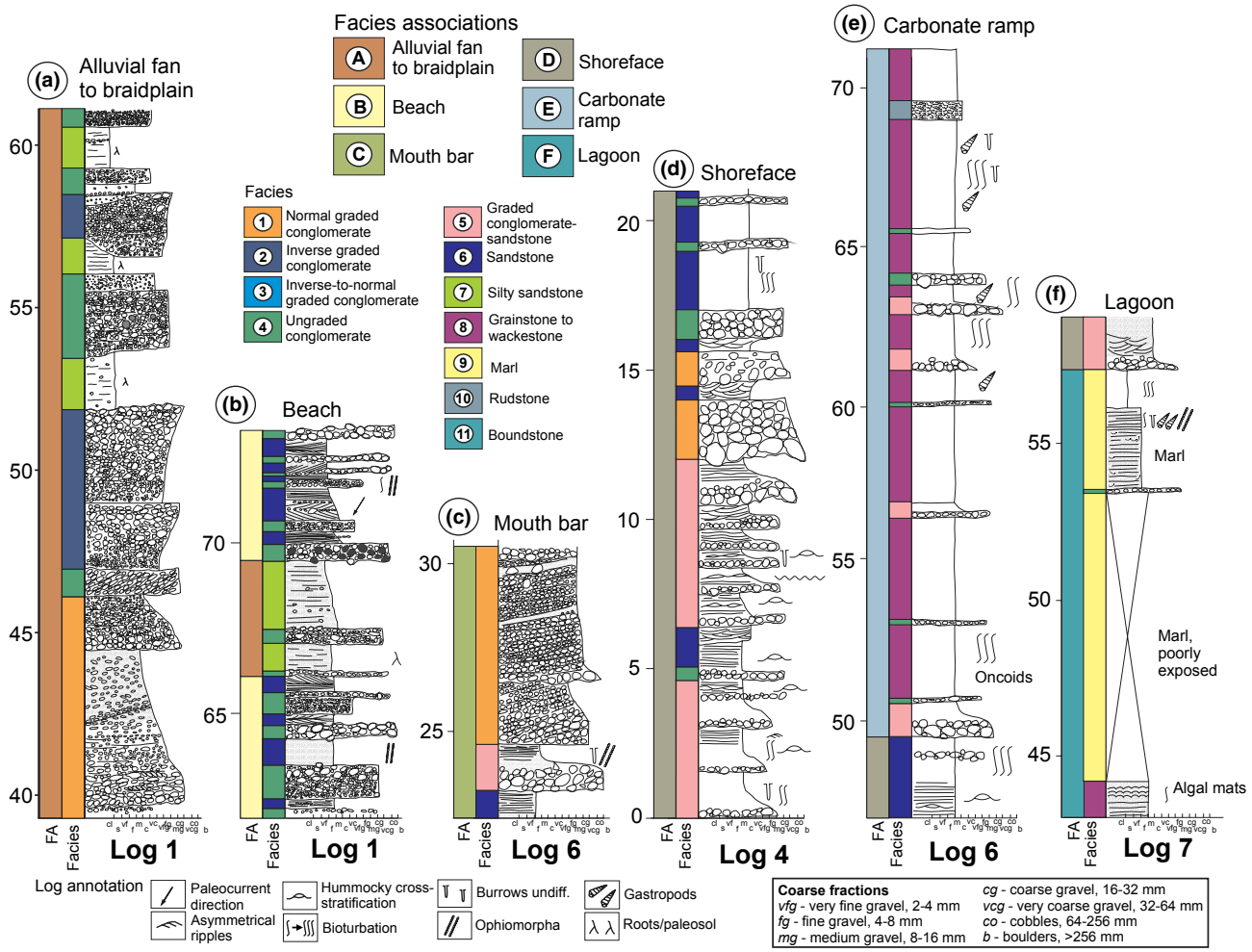

FIGURE 6 Typical sedimentary log expression for facies associations in the Bandar Jissah Basin. Facies are defined in Table 1

less possibilities for significant avulsions as compared to more proximal parts of the alluvial fan. This allowed for development of thicker and more laterally extensive paleosols.

4.1.2 | FA B

Description

FA B consists of Facies 4.4 and 6, differing in grain size but both displaying a high textural maturity and well-developed parallel laminations and low-angle cross-stratification (Table 1; Figures 6 and 7b). Facies 4.4 consists of parallel bedded to low-angle cross-stratified well-rounded and sorted fine quartz gravel. It overlies grainstones to wackestones (Facies 8) and is overlain by bioturbated sandstones (Facies 6). Facies 6 consists of very fine to coarse sand displaying sedimentary structures such as parallel lamination and ripple- to dune-scale cross-stratification that reflect a variety of oscillatory, bidirectional and unidirectional current regimes. Facies 6 sandstones have a variable content of skeletal fragments and *Ophiomorpha* trace fossils.

Interpretation

We interpret FA B as beach deposits with significant differences in grain size and identifiable structures; Facies 4.4 represent a gravel beach deposit on the basis of its sedimentary structures, unusually high textural maturity and stratigraphic context. Parallel lamination in Facies 6 sandstones is indicative of upper flow regime typical for the foreshore/swash zone (Clifton, Hunter, & Phillips, 1971). We are not able to support this interpretation with observations of marine fauna. However, we note that the preservation potential for body fossils in such a depositional environment is inherently low.

4.1.3 | FA C

Description

FA 3 consists of (a) conglomerates that are normal graded (Facies 1), inverse-to-normal graded (Facies 3) and non-graded (Facies 4.2 and 4.3) and (b) normal graded conglomerate to sandstone (Facies 5) (Table 1; Figures 6 and 7c). The

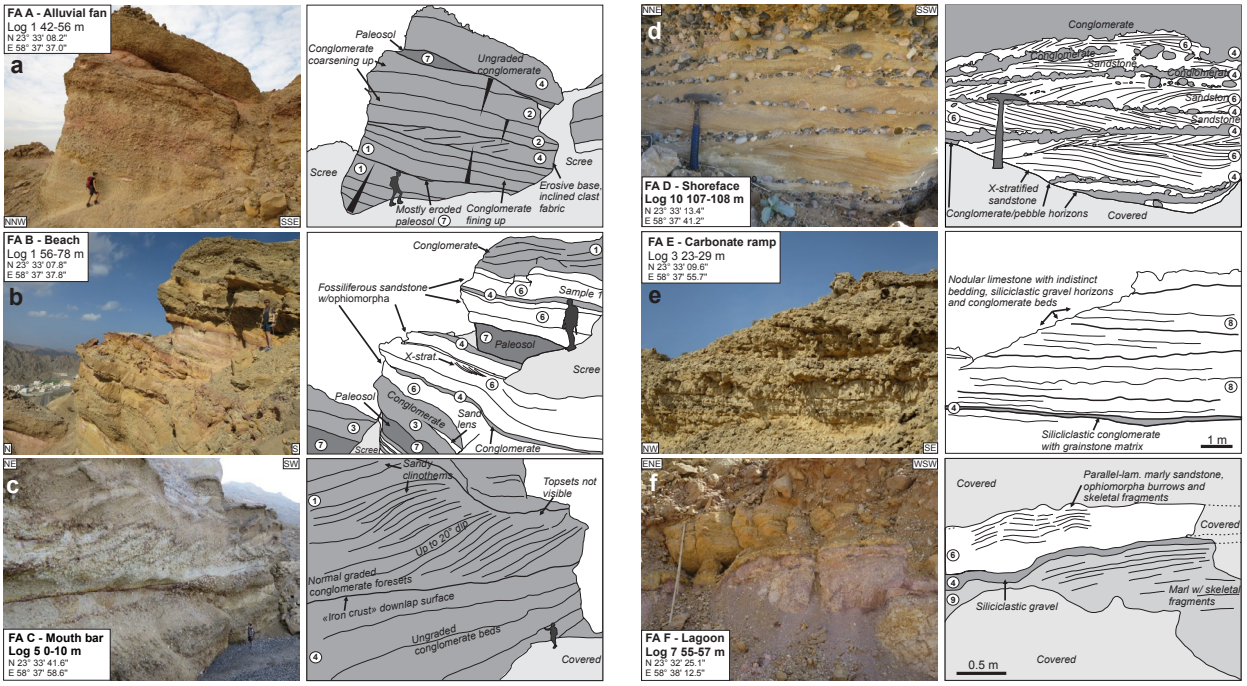

FIGURE 7 Typical field expression of facies associations defined for this work. Numbers refer to facies defined in Table 1. Note different scales and outcrop quality

bedding and clast fabric display steep (up to 20 degrees) tangential foresets (1–6 m heights) and alternations between conglomeratic and sandy clinothems are common (Figure 7c). The conglomerates are mostly clast-supported with a fine-grained matrix of sandstones (Facies 6) and/or grainstones to wackestones (Facies 8). Sedimentary structures in sandstones (Facies 6) sandstones include parallel lamination, asymmetric ripples, trough-, sigmoidal-, herringbone- and hummocky cross-stratification, mud drapings on parallel laminae and cross-sets, and *Ophiomorpha* trace fossils.

Interpretation

FA C represents conglomeratic mouth bar/delta front deposits in a carbonate-producing marine basin. Shallow water is indicated by modest foreset heights (e.g. Patruno, Hampson, & Jackson, 2015), but a lack of well-preserved topsets prevents further quantification of paleowater depth. Coarse siliciclastic conglomerates deposited from high-density turbidity currents and subaqueous mass flows establish FA C as a marine equivalent of FA A; the marine affiliation is suggested by the grainstones to wackestones (Facies 8) matrix of conglomerates, *Ophiomorpha* trace fossils and a bimodal current regime reflected in the sedimentary structures. Interbedded conglomeratic and sandy clinothems indicate flow separation as different flows (streamflows, debris flows) met standing water (e.g. Bhattacharya, 2006). The subsequent decrease of viscosity and sediment concentration led to increased runout and deposition of tangential foresets. Preservation potential for FA C relates to fluvial discharge and the nearshore energy regime. During periods of low fluvial discharge, carbonate production was active and fine-grained siliciclastic deposits were reworked by wave- and tidal currents.

4.1.4 | FA D

Description

FA D consists of relatively fine-grained sediments (Facies 6 and 8) with the exceptions of the rudstones and boundstones of Facies 10 and 11, respectively (Table 1; Figures 6 and 7d). The sediment composition varies from fully siliciclastic (Facies 6) to fully carbonate ("clean" Facies 8, Facies 10 and 11). Bioturbation is extensive, particularly in grainstones to wackestones (Facies 8), where most primary structure is obliterated and bedding surfaces are vague to indiscernible. *Ophiomorpha* trace fossils are common, *Thalassanoides* are less frequently observed. Where preserved, primary sedimentary structures include plane parallel laminations, asymmetrical ripples, tangential-, trough-, low-angle- and hummocky cross-stratification on a variety of scales from cm-scale cross-lamination to m-scale dune cross-stratification. Bidirectional current indicators include herringbone cross-bedding and double mud drapes (Figure 7d). Paleocurrent measurements give sediment transport directions with a spread of 215 degrees from NW to S. Body fossils and skeletal fragments are common with echinoids, gastropods, bivalves, and scattered coral fragments and calcareous red algae identified. Grainstones to wackestones (Facies 8) are dominated by

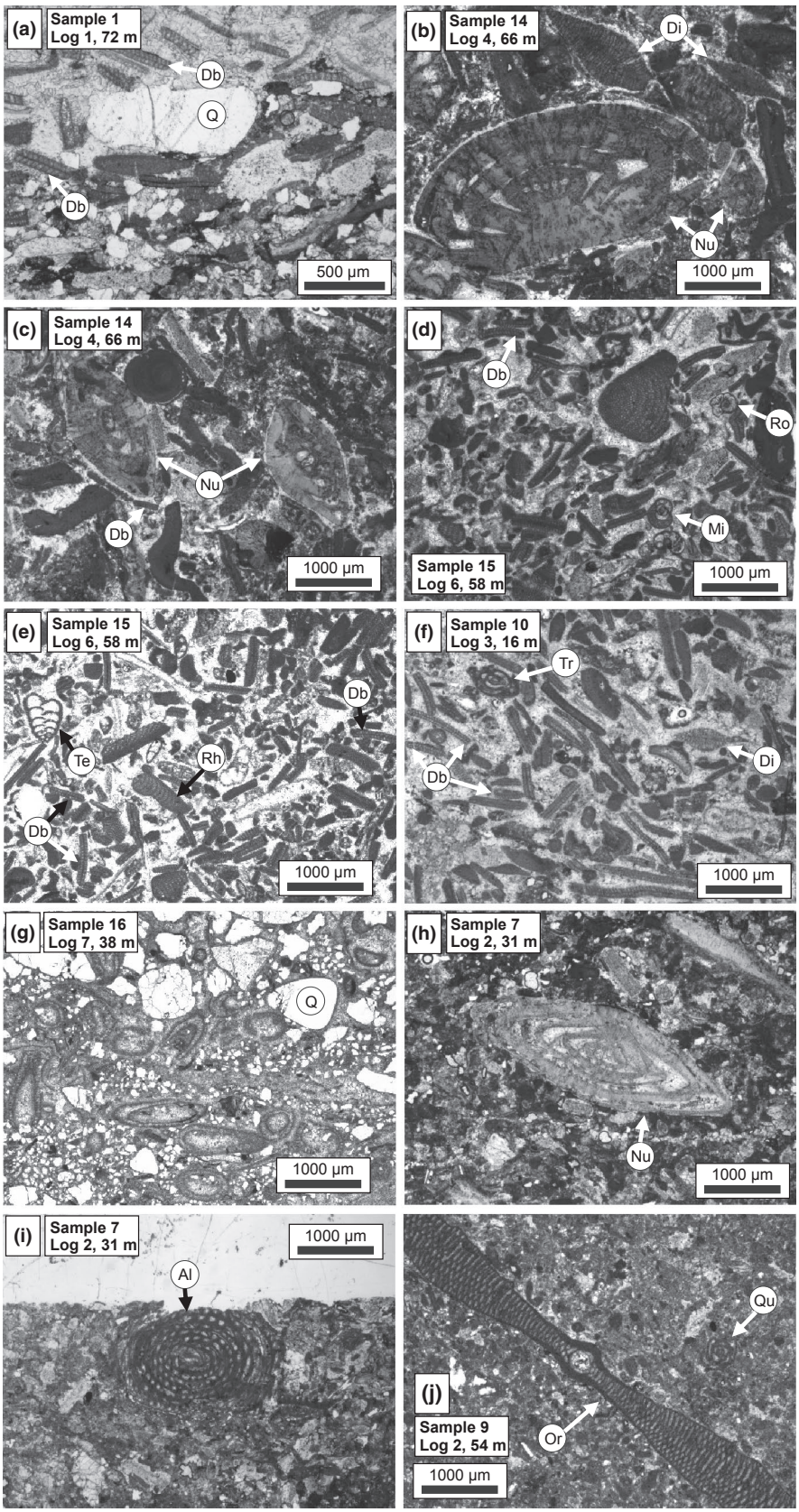

FIGURE 8 Thin sections from the late Paleocene to Eocene mixed siliciclastic-carbonate succession of the Bandar Jissah Basin. This sections display variation from medium to coarse grained fossiliferous calcareous sandstone (a) and wackestone (i and j) and grainstone (b, c, d, e, f and h). The fossil assemblage is dominated by larger benthic foraminifera and calcareous algae. See Figure 5 for sample locations. Db – *Distichoplax biserialis,* Di – *Discocyclina,* Nu – *Nummulites,* Al – *Alveolina,* Te – *Textularia,* Rh – *Rhabdorites,* Ro – *Rotalia,* Mi – *Miliodae,* Tr – *Triloculina,* Or – *Orbitolites,* Qu – *Quinceloculina,* Q – *Quartz*

larger foraminifera such as *Nummulites*, *Alveolina*, miliolids, *Discocyclina* and *Orbitolites*, and the calcareous algae *Distichoplax biserialis* (Figure 8). Increasing karstification is observed towards the southwest.

Interpretation

FA D represents a shoreface environment in which the sediment was affected by waves and tidal currents. Further differentiation can be inferred from the specific sedimentary structures observed; hummocky cross-stratification is representative for offshore transition/lower shoreface whereas low-angle- and trough cross-stratification and asymmetrical ripples suggest an upper shoreface setting (e.g. Clifton, 2006). The rate of carbonate to siliciclastic grains relate to fluvial discharge and position with regards to shoreline. The increased karstification towards the southwest suggests a position near the shoreline, which suggests a strong influence of relative sea level fluctuations.

4.1.5 | FA E

Description

FA E consists of graded conglomerate – sandstone (Table 1; Facies 5), grainstones to wackestones rich in benthic foraminifera and calcareous algae (Facies 8), rudstone (Facies 10), boundstone (Facies 11) and silty sandstone (Facies 7; Figures 6 and 7e). Bioturbation has destroyed most primary sedimentary structures to the point where even bedding planes are vague and difficult, if not impossible, to correlate through the basin (Figure 7e). Isolated pockets of less bioturbated FA E rocks display parallel lamination, low-angle cross-stratification and trough cross-stratification. Facies 8 deposits display foresets with heights up to 2 m at one locality (Log 9). Rudstone beds consist of gastropods, coral fragments, larger foraminifera and thick, broken oyster tests. Rudstone and coral boundstone beds are generally thin (<1 m) and localized. An exception of this is a tens of meters thick coral aggregate near the Yiti Beach Fault (Figure 9c). Foraminiferal content varies but individual beds or bedsets tend to be dominated by similar species. FA E is frequently karstified (dm-scale) in the southwest, where karstified surfaces are often observed together with paleosols (Facies 7). Paleosols (Facies 7) are also observed occasionally towards the northeast (log 20).

Interpretation

We interpret FA E as the shallow part of a carbonate ramp on the basis of the complete bioturbation, proximal position with regards to the shoreline suggested by siliciclastic content and karstification, scattered nature of coral reefs and reef mounds, few abrupt lateral facies changes and migrating, possibly wave-breaking bars. Reefs and mounds indicate periods of high carbonate productivity, little siliciclastic sedimentary input and/or an elevated bathymetric position (e.g. uplifted footwall high) that favour carbonate production while inhibiting siliciclastic input (e.g. Cross & Bosence, 2008; Dorobek, 2008). The carbonate ramp was storm-affected, as suggested by grainstones (Facies 8) interbedded with tempestites (Facies 5 normal graded conglomerate – sandstone/grainstone). Bathymetric variations on the carbonate ramp can also result from shoreward sediment transport during storms, resulting in deposition of barrier complexes. These positive bathymetric features favoured carbonate production/reef development. The shallow water associated with these features brought about a sensitivity to sea-level variations; paleosols (Facies 7) developed on the barrier complexes during periods of low relative sea level. Rudstones with thick-tested oysters indicate an agitated depositional environment related to wave-action in the barrier complex (Racey, 1995). Occurrence of coral fragments in grainstones indicates proximity to reef mounds. The limited continuity and thickness of rudstones (Facies 10) and boundstones (Facies 11) favour the interpretation of a sediment-driven barrier complex over a tectonically induced high bathymetric position. Foraminiferal content indicates a variety of water depths (shallower – *Alveolina*, deeper – *Nummulites*), energy regimes (miliolids – low energy), environmental stress (low vs. high-diversity fauna) and vegetation on the seabed (*Orbitolites* indicate vegetation; Figure 8). The nearly complete bio-retexturing of the sediment has previously been ascribed to seagrass roots and rhizomes, annelid seaworms and other burrowing organisms such as echinoids (Beavington-Penney et al., 2006). Karstification in the southwestern area might relate to tectonically driven accommodation adjustments (slip events in basin-controlling faults).

4.1.6 | FA F

Description

FA F consists of foraminiferal grainstones to wackestones (Facies 8), marl (Facies 9), rudstone (Facies 10) and boundstone (Facies 11; Table 1; Figures 6 and 7f). Generally, the sediment lacks primary sedimentary structures due to extensive bioturbation, however plane-parallel lamination, low-angle- and trough cross-stratification is preserved in places. The grainstones are dominated by larger foraminifera, with guest appearances by gastropods, echinoids, oysters and coral fragments and contain a variable proportion of siliciclastic grains. The body fossils described above are either encased in a foraminiferal grainstone/packstone/wackestone matrix or concentrated in rudstones. Beige to dark red marl (Facies 9) is littered with gastropods and undifferentiated shell fragments and displays distinct *Ophiomorpha* burrowing.

Interpretation

We interpret FA F as lagoonal deposits, particularly because of the combination between rudstones and lagoonal

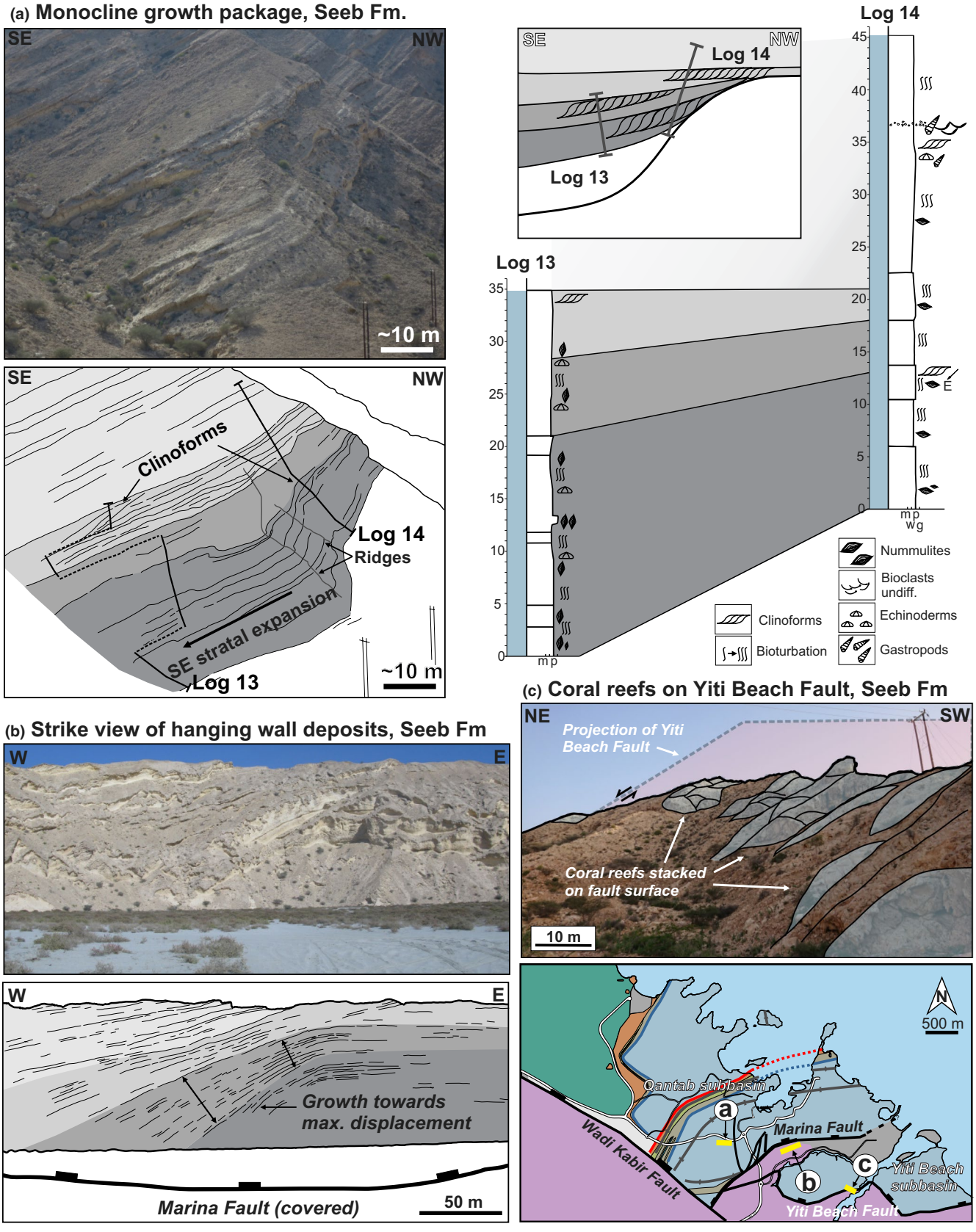

FIGURE 9 Seeb Formation carbonate growth sections in the Qantab subbasin. (a) Lower Seeb Formation growth package in Qantab subbasin monocline with supporting logs and proposed model. (b) Upper Seeb Formation growth packages as seen along strike in the immediate hanging wall of the Marina fault. Strata expand towards inferred local displacement maximum. (c) Coral reefs stacking on Yiti Beach Fault

marls, which has previously been described for the Rusayl Formation by Racey (1995). Calm conditions prevailed with stormy interruptions resulting in trough cross-stratification of wackestones to grainstones. Upon first sight, Facies 9 marls are strikingly similar to Facies 7 paleosols, however, the fossil assemblage and *Ophiomorpha* trace fossils strongly indicate a marine origin. Occasional occurrences of algal mats indicate elevated salinity levels (e.g. Paerl, Pinckney, & Steppe, 2000).

4.2 | Basin structures

The Banurama Detachment and Wadi Kabir, Marina and Yiti Beach faults are fundamental structures in the Bandar Jissah Basin. The Wadi Kabir Fault is considered part of a regional range-front fault complex (Braathen & Osmundsen, 2020; Mattern & Scharf, 2018). Also of significance for this study is the Qantab subbasin monocline, which is refolded in a roll-over fold in the hanging wall of the Marina Fault (Figures 2b and 3d).

4.2.1 | Banurama Detachment

The Banurama Detachment is exposed near the southeastern end of the Wadi Al Kabir urban area, as a klippe in the footwall of the Wadi Kabir Fault and in a down-faulted block/lens within this fault. It is inferred below the Paleogene basin fill in the hanging wall of the Wadi Kabir Fault (Figure 2). In the Wadi Kabir Fault footwall, the sub-horizontal Banurama Detachment separates steeply NE-dipping Triassic marbles in the footwall from 40–60° SW-dipping Paleogene strata (Jafnayn Fm) in the hanging wall (Figure 4). These dips are comparable to dips of Paleogene strata in the juxtaposed Wadi Kabir Fault hanging wall basin (Figure 4d; Wessels, 2012). Furthermore, the Paleogene strata display a depositional contact with mildly sheared ophiolites on both sides of the Wadi Kabir Fault. The Banurama Detachment constitutes a 20–30 m thick section of fault rocks, which include serpentine-talc phyllonites and cataclasites hosting clasts of magnesite, all with ophiolite affinity, overlying mainly marble breccias of footwall affinity. Within this zone, which has a semi-brittle to brittle style, most primary rock characteristics are erased, with strain diminishing towards the margins. The fundamental shear boundary between rocks of ophiolite affinity (footwall) and deformed sediments (hanging wall), where exposed, is approximately 10 cm thick, overlain by a few meters of highly strained sediments. The shear zone shows extensive folding of partly intact rock coupled with cm to dm-wide shear zones hosting typical brittle fault rocks, many with signs of plastic deformation elements (particularly associated with serpentine-talc formation; Figure 4c). Many shear zones host slip surfaces (slickensides; Figure 4b). There is consistent top-NNE (ca. 030°) tectonic transport in the Banurama Detachment and shear zones within the core complex as indicated by slickenlines and stretching lineations and reported by previous workers and in our data (see Ruwi-Yiti-Yenkit shear zone in Figure 2b; e.g. Braathen & Osmundsen, 2020; Jolivet, Goffé, Bousquet, Oberhänsli, & Michard, 1998; Warren & Miller, 2007). A minimum displacement of ~1,500 m on the Banurama Detachment is estimated by measuring the length of the outcrop in a direction parallel to tectonic transport (~750 m) and considering that the detachment cuts the bedding at 45°. Judging from the rotation of strata and thickness of the detachment, however, the displacement is likely significantly larger.

4.2.2 | Wadi Kabir Fault

The NW-SE striking, steeply NE-dipping Wadi Kabir Fault is the most conspicuous structure in the Bandar Jissah Basin, expressed as a 50–200 m tall rock face readily mappable from Ruwi to ~1 km SW Wadi Aday (Figures 2 and 3). The Wadi Kabir Fault cuts the Banurama Detachment, as suggested by the steep and comparable dips of Paleogene strata on either side of the Wadi Kabir Fault, and the presence of the Banurama Detachment in a rider block within the Wadi Kabir Fault (Figure 4d). Paleogene sedimentary rocks and the Banurama Detachment is only preserved in a limited area in the footwall of the Wadi Kabir Fault. Hence, in the present-day landscape the Wadi Kabir Fault mainly separates Paleogene sediments in the hanging wall from Triassic low-grade marbles in the footwall (Le Métour et al., 1992). The Wadi Kabir Fault is characterized by a few meters of mildly consolidated fault rock layers of the breccia series (sensu Braathen, Osmundsen, & Gabrielsen, 2004) that follow the bedding of footwall marbles. Fault rocks include marble breccias overlain by ophiolite breccias towards the hanging wall. Slickenlines on the composite principal slip surface and proximal footwall damage zone display dip-slip kinematics with a slight sinistral component. A subordinate population of slickenlines suggests oblique-slip, normal-sinistral kinematics late in the fault evolution.

4.2.3 | Marina fault

The Marina Fault extends SE from a recently constructed marina between the Barr Al Jissah peninsula and Yiti Beach to where it merges with the Wadi Kabir Fault in the west. It displays normal down-to-NW movement with Triassic-Jurassic marbles in the footwall and the Eocene Seeb Formation in the hanging wall. The Marina Fault is characterized by a narrow zone (5–10 m) of marble cataclasites and tectonic lenses of

footwall affinity. Strata in the immediate hanging wall dip toward NW and consist of footwall-derived clasts floating in a matrix of fossiliferous wackestones. The Marina Fault is associated with sedimentary growth packages in the upper Seeb Formation (Figure 9).

4.2.4 | Qantab subbasin monocline

A basin-scale ENE-WSW trending monocline is observed in the hanging wall of the Marina and Wadi Kabir faults. The informally named Qantab subbasin monocline displays a non-systematic distribution of bedding orientations suggesting non-cylindrical folding (Figure 2b). The most prominent trend fits a moderately ESE-plunging axis, another trend a sub-horizontal ENE axis. Notably, the first trend is perpendicular to the kinematic axes of shear zones in the footwall core complex and the Banurama Detachment (Braathen & Osmundsen, 2020), conforming to an interpretation of the basin as a supradetachment half-graben. The distinct plunge of the ESE trending fold-axis can be compared to moderate bedding dips in the proximal hanging wall of the Marina Fault, consistent with rotation of the hanging wall block including the Qantab subbasin monocline during movements on this fault. A WSW-ENE Marina Fault trend parallels the less prominent ENE fold axis suggested by bedding data. The Qantab subbasin monocline is associated with sedimentary growth packages expanding towards the southeast, suggesting syn-depositional (Rusayl and Seeb formations) growth of the monocline (Figure 9).

4.2.5 | Yiti Beach fault

The Yiti Beach Fault marks the southern boundary of both the Yiti Beach subbasin and the Bandar Jissah Basin. The Yiti Beach Fault zone is an approximately 15–20 m thick zone of semi-brittle phyllonites topped by brittle fault breccias, all with footwall affinity. The fault zone has an overall moderate (~45°) northerly dip, and separates Jurassic-Triassic schists and marbles of the footwall from moderately south-dipping Eocene beds (Seeb Formation), including stacked coral reefs, in the hanging wall. Stretching lineations and slickenlines suggest normal, down to the NNE to NNW kinematics on the fault zone (Figure 2).

5 | TECTONOSTRATIGRAPHIC DEVELOPMENT

The Bandar Jissah Basin is characterized by a two-fold tectonic evolution reflected in lateral and vertical facies architecture variations of the basin fill. The Banurama Detachment controlled the initial basin development before it was rotated, deactivated and cut by the Wadi Kabir Fault as steep faults became active and generated rift-style subbasins. The timing of activity on the Banurama Detachment is given by the ages of strata that were rotated before being cut by the Wadi Kabir Fault. The upper Paleocene to lower Eocene Jafnayn Formation was deposited in a supradetachment basin controlled by the Banurama Detachment. Broad uplift-subsidence patterns following displacement in the Banurama Detachment gave a gradual proximal-to-distal facies transition from south to north. Facies distributions and stratal geometries in the Rusayl and Seeb formations, however, are more complex, reflecting the transition from a supradetachment basin to a rift-style basin system. Below, we subdivide the tectonic evolution of the Bandar Jissah Basin into three phases based on the structural chronology and spatio-temporal stratigraphic trends.

5.1 | Supradetachment basin phase: Jafnayn Formation – late Paleocene to early Eocene

The lowermost basin fill is characterized by a series of prograding coarse clastic wedges of the Jafnayn Formation deposited onto the ophiolitic substrate. Deposition of alluvial fan to braidplain deposits (FA A) was punctuated by rapid transgressions with deposition of beach (FA B), mouth bar (FA C), shoreface (FA D) and/or carbonate ramp (FA E) onto alluvial fans. The prograding wedges display a strong south-to-north proximal-distal trend, reflecting depositional gradient, shoreline proximity and depositional processes (Figure 10). The proximal deposits are continental and consist of alluvial fan conglomerates grading downdip into coarse braidplain deposits (FA A; Figures 10 and 3, logs 1 and 10). A gradual transition from alluvial fan to braidplain deposits is reflected by (a) increasingly organized bedding, suggesting gradually more turbulent flow types, (b) increasing prevalence of fining-upwards conglomerate beds, typical for fluvial deposits and (c) thicker and more spatially extensive paleosols, reflecting a run-off pattern confined to channel belts, allowing paleosols to establish on the floodplains (Figure 3, logs 1 and 10). Braidplain deposits (FA A) grade into shallow marine deposits; conglomeratic mouth bars (FA C), beach sands (FA B), shoreface deposits (FA D) and ultimately carbonate ramp deposits with variable siliciclastic content (FA E; Figure 10). The shallow marine deposits vary according to shoreline morphology and position with respect to the shoreline and river mouths, demonstrating a dominance of fluvial, wave or tidal processes at different stratigraphic levels and positions both laterally along the paleo-shoreline and along the proximal-distal axis.

Shoreline transgressions led to deposition of shallow-marine deposits (FA B, C, D, E) onto continental deposits. The lack of convincing evidence for extensive transgressive reworking during flooding suggests shoreline transgressions were rapid, reflecting high accommodation rates, possibly

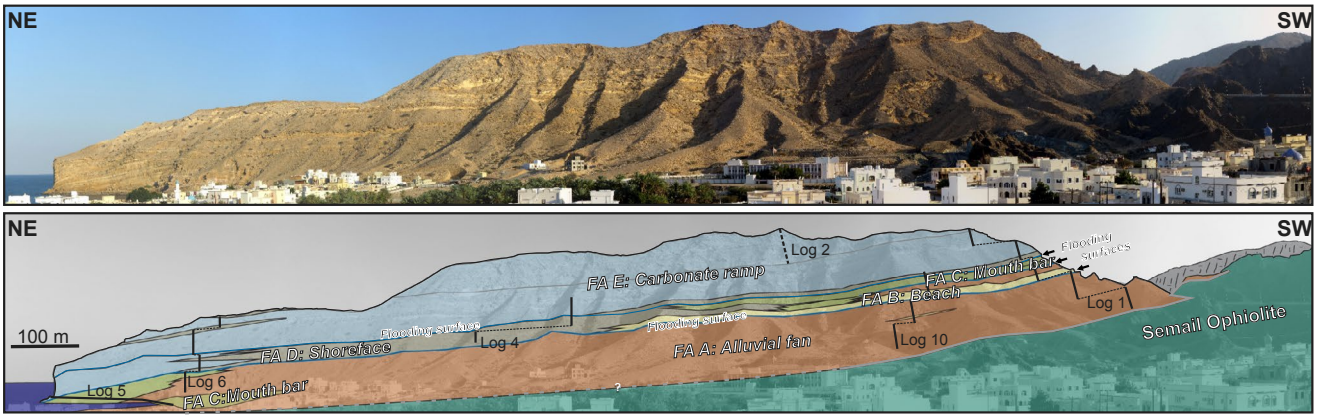

FIGURE 10 Panorama showing facies association distributions in the Jafnayn Formation in Qantab with annotated log traces. See Figure 2b for location

related to slip events in faults controlling accommodation, likely the Banurama Detachment. The transgressive development from alluvial fans to fan delta, shoreface and carbonate ramp is similar to supradetachment basin characteristics in the Dolomites as documented by Massari and Neri (1997).

The only preserved Paleogene sediments in the footwall of the Wadi Kabir Fault are located NW of the Bandar Jissah Basin, and thus are not directly comparable. Nevertheless, we argue that observations from this Paleogene outlier are fundamental for understanding stratigraphic development in the Bandar Jissah Basin (Figure 2). The Banurama Detachment is described both at the base of the ophiolite in the footwall of the Wadi Kabir Fault and in a rider block along the Wadi Kabir Fault, suggesting the Wadi Kabir Fault post-dates the Banurama Detachment (Figure 2d). Moreover, similar rotation of Paleogene strata in both the hanging wall and footwall of the Wadi Kabir Fault indicate that the Banurama Detachment controlled basin morphology during deposition of the Jafnayn Formation (Figure 4d). Continued control of the Banurama Detachment on basin evolution is evidenced by sedimentary growth packages at higher stratigraphic levels (lower Seeb Formation) in the Qantab Subbasin monocline. We classify the Bandar Jissah Basin as a supradetachment basin during deposition of the Jafnayn Formation, which displays strong similarities with generalized supradetachment basin successions (Figure 1; Friedmann & Burbank, 1995): Firstly, sedimentary transport directions (NNE-NNW) in alluvial fan to braidplain conglomerates compare with tectonic transport directions in the Banurama Detachment (top-NNE) (Figures 2 and 3). Secondly, the spectrum of coarse subaerial debris flow to high-energy streamflood deposits in the Qantab subbasin indicates a high-relief source area in the south. This is consistent with large-magnitude footwall uplift (isostatic compensation) following displacement in the Banurama Detachment, and perhaps deeper detachments within the Saih Hatat window (Braathen & Osmundsen, 2020; Warren & Miller, 2007). A southerly sediment source also conforms to a Maastrichtian to Paleocene uplift of the Saih Hatat window, as documented by Hansman et al. (2017). Finally, continental deposits in extensional basins indicate limited accommodation near the controlling fault. This is typical for supradetachment basins where deposition of footwall-derived strata takes place in distal positions with respect to the fault (Friedmann & Burbank, 1995).

Steep dips (~40–60°) of originally (sub)horizontal Paleogene carbonates above the Banurama Detachment in the Wadi Kabir Fault footwall suggests that the detachment initiated as a steep fault before being rotated together with its hanging wall basin, likely as an isostatic response to faulting. Considerations around whether the studied supradetachment basin system can be classified as a breakaway basin or a ramp basin (sensu Vetti & Fossen, 2012) are difficult for several reasons; (a) limited exposure of the Banurama Detachment, constrained to a rider block and the footwall of the Wadi Kabir Fault, (b) no outcrops of the supradetachment basin further inland and (c) a lack of suitable sub-surface data offshore the study area. The tectonic contact between the Paleogene carbonates and Banurama Detachment, which initiated as a steep fault, might suggest that the sediments were deposited in a breakaway basin. However, we recognize that other mechanisms can have placed the Paleogene sediments in contact with the detachment (see e.g. Asti et al., 2019). Hence, a classification of the studied supradetachment basin system will be highly uncertain. Beach sands (FA B) between the two lowermost alluvial fan packages (FA A) in the Qantab subbasin (Figure 5 - log 1; Supplementary Material) contain the calcareous algae *Distichoplax biserialis,* which constrains the age of the lowermost basin fill and onset of accommodation generation in the Bandar Jissah Basin to the late Paleocene to Eocene (Figure 8a; Denizot & Massieux, 1965; Dietrich, 1927; Pia, 1934). *Distichoplax biserialis* been have also been recorded in Jafnayn Formation deposits of the nearby Sunub Basin (Mattern & Bernecker, 2018). Accumulation of

sediments in extensional basins around the Saih Hatat metamorphic core complex have been reported to commence in the Late Cretaceous (e.g. Abbasi et al., 2014; Braathen and Osmundsen, 2020; Mann et al., 1990; Nolan et al., 1990). Accordingly, we speculate that the lack of Upper Cretaceous sediments in the Bandar Jissah Basin is related to the position with regards to the Saih Hatat metamorphic core complex. Here, isostatic uplift following large-magnitude detachment faulting limited accommodation space near the detachment and progressively cannibalized earlier supradetachment basin sediments with each uplift episode.

Flooding, possibly driven by basin subsidence following slip events in the controlling detachment, led to carbonate ramp (FA E) deposition over the coarse siliciclastic wedges (Figure 10). Wackestones to grainstones with fluctuating amounts of quartz grains, pebble horizons and conglomerate interbeds suggest that carbonate production persisted even with significant terrigenous input to the basin. We attribute this to the coarse nature of the siliciclastic input, which has previously been suggested to have limited detrimental effects on carbonate production (Cross & Bosence, 2008; Friedman, 1988). FA E limestones in the Jafnayn Formation are completely bio-retextured with a nodular appearance, weak to indiscernible bedding surfaces and only occasional and locally preserved primary sedimentary structure (Figure 6). Bathymetric variations are evident from shallower-water facies (barrier system) in distal positions; wave-breaking gravel bars, oyster banks, and coral reefs (facies 5, 10, 11). Karst surfaces (facies 8) in log 9 constrain the extent of the Qantab subbasin on the carbonate ramp (Figure 5 – log 9, 3; Supplementary Material). Fault-driven local facies variations on the carbonate ramp present an alternative explanation for shallow-water facies and subaerial exposure of more distal parts of the ramp (e.g. Massari & Neri, 1997). Without evidence of such faults, however, we recognize that these shallow marine to continental facies likely result from shoreward transport of sediment during storms that affect the carbonate ramp. Sediments accumulate to form barrier complexes on which reefs may develop, but which are also sensitive to sea level falls. The modest lateral extent and thickness of bars, mounds and reefs (log 9) provide additional support for this interpretation.

5.2 | Early transition phase: Rusayl Formation – early to middle Eocene

The boundary between the Jafnayn and Rusayl formations in the Qantab subbasin represents unconformable deposition of continental conglomerate (FA A) over the carbonate ramp (FA E), corresponding with other observations in the region (Figures 3 and 5 – log 21; Supplementary Material; Nolan et al., 1990; Özcan et al., 2016). The Rusayl Formation's basal alluvial fan grade upward into fan delta (FA C) and shoreface deposits (FA D) affected by tidal currents (Figure 7). The shoreface assemblage consists of alternating siliciclastic conglomerate and mixed carbonate-silicliclastic tidally influenced sandstone (Figure 7). Paleocurrent data from gravelly foresets indicate an overall sedimentary transport towards east, with some sandstone cross-sets indicating bidirectional ~N-S currents (Figure 3). The dominantly easterly sedimentary transport is perpendicular to the Qantab subbasin monocline, contrasting the northerly transport recorded in the Jafnayn Formation and emphasizing influence by initial monocline growth. The monocline was active during deposition of the Rusayl Formation and lower Seeb Formation. Together with associated growth packages, the monocline closely resembles structures and sedimentary architectures from the Suez rift, where syn-sedimentary fault-propagation folding was documented by Sharp, Gawthorpe, Underhill, and Gupta (2000). Here, however, we lack observations of blind faults within the monocline. Additionally, the most prominent trend obtained from bedding orientations in the monocline indicates an ESE-trending fold axis, which is perpendicular to tectonic fabrics on the Banurama Detachment (Figure 2b). Hence, we suggest that monocline growth during deposition of the Rusayl and lower Seeb formations represents rollover folding related to the geometry of, and movement on, the underlying Banurama Detachment rather than being affiliated with the Marina Fault at this stage. We relate backstepping of the Rusayl Formation alluvial fan (FA A), as indicated by the upward grading into fan-delta (FA C) and shoreface deposits (FA D), to increasing accommodation rates east of the monocline (Figure 5 – logs 21 and 7; Supplementary Material). The shoreface package shows an initial upward thinning and fining of conglomerate beds before conglomerates again grow thicker and more frequent, indicating shoreline retreat and advance, respectively (Figure 5 – logs 21 and 7; Supplementary Material). The overlying sediments indicate shoreline regression, accumulating as lagoonal (FA F), beach (FA B) and upper shoreface (FA D) deposits (Figure 5 - log 7; Supplementary Material).

5.3 | Late transition to rift-style basin phase: Seeb Formation – middle Eocene

The base of the Seeb Formation records a major flooding event that resulted in deposition of a thick ramp-type carbonate succession with scattered gravel beds (FA E) onto the more proximal Rusayl Formation (Figures 3 and 5 – logs 2, 8, 13, 14, 19; Supplementary Material). The south-to-north proximal-distal trend recorded in the Jafnayn Formation is readily identifiable also in the Seeb Formation; distal sections consist of relatively clean carbonates dominated by well-preserved larger benthic foraminifera (*Alveolina, Nummulites*) and lack evidence for

subaerial exposure (Figure 5 - logs 8 and 2; Supplementary Material). Proximal sections, on the other hand, display more abraded skeletal fragments and abundant karst surfaces, paleosols and siliciclastic gravel to cobble conglomerates (Figure 5 – logs 15 and 19; Supplementary Material), emphasizing the marginal marine setting. Significant run-off from hinterland catchments upon deposition of the Seeb Formation is further indicated by a series of fining-upwards siliciclastic conglomerate beds (facies 1 and 5) in the southern corner of the Qantab subbasin (Figure 5 - log 19 and 15; Supplementary Material). Modifications to the overall northerly accommodation increase resulted from displacement, first on the Banurama Detachment with associated inception of the Qantab subbasin monocline and subsequently on the Marina Fault, fitting the suggested chronology of the monocline. Growth packages in the Qantab subbasin monocline in the lower Seeb Formation, display thickness increase and progradation of nummulitic limestone foresets towards the east (Figure 9a). This growth package documents the syn-sedimentary relevance of the Qantab subbasin monocline, which became active during deposition of the Rusayl Formation. Another growth package succession is recorded in the upper Seeb Formation, located in the immediate hanging wall of the Marina Fault, which display stratal expansion towards the inferred maximum displacement on this fault (Figure 9b). Displacement in the Marina Fault tilted hanging wall strata, resulting in the gentle east to south stratal dips observed throughout the Qantab subbasin (Figure 3). This agrees with the interpretation of both the ESE-plunge of the detachment-related fold axis and the sub-horizontal ENE trend that is parallel to the Marina Fault (Figure 2b). The reduction of siliciclastic material in the upper Seeb Formation, particularly in distal (northerly) positions, relate to the transition from supradetachment to rift-style setting, with (a) less footwall rebound and thus smaller and lower-relief footwall catchment areas and (b) increasing near-fault accommodation (Figure 1). The Marina Fault likely merged with or was cut by the Wadi Kabir Fault in the southern corner of the Qantab subbasin. No Paleogene strata are preserved in the Wadi Kabir Fault footwall in this position. Coarse shallow marine siliciclastic conglomerates (FA D) in the upper Seeb Formation, deposited in the proximal hanging wall near the junction between the two faults, suggest a relay zone between the two faults existed during deposition, feeding sediments into the basin. This relay zone promoted sediment transport from the footwall to the hanging wall basin and a structurally high position in the hanging wall conforms to deposition of hinterland-derived conglomerates in a shallow marine setting. Accordingly, we propose that both the Wadi Kabir Fault and Marina Fault were active at this time. This is supported by the component of sinistral oblique-slip documented for the Wadi Kabir Fault (Figure 2b).

We suggest that the deposits in the Yiti Beach subbasin belong to the Seeb Formation, contradicting Le Métour et al. (1992), who interpreted these sediments as part of the Jafnayn Formation (Figure 2c). We observe plentiful nummulitic limestones and coral reefs in the Yiti Beach subbasin that match well with previous descriptions of the Seeb Formation (Nolan et al., 1990) and facies of the Seeb Formation in the Qantab subbasin. Displacement on the Yiti Beach Fault established the Yiti Beach subbasin as a half-graben basin where it controlled accommodation development during deposition of the upper Seeb Formation. Coral reefs grew on the Yiti Beach Fault surface to form large, vertically stacked reef complexes, suggesting increasing water depth in the hanging wall of the fault, likely driven by fault slip events (Figure 9c). This fault-generated bathymetry led to deposition in distinct facies belts in the Yiti Beach subbasin; in-situ reefs and reef debris grade basinward into skeletal wackestones. With in-situ reefs and no observations of other exotic clasts in the hanging wall basin, we suggest the Yiti Beach Fault footwall was subaerially exposed without significant drainages delivering sediment across the fault scarp during deposition of the Seeb Formation in the Yiti Beach subbasin.

The inception and growth of the Wadi Kabir, Marina and Yiti Beach faults could reflect a changing stress-regime that triggered new faults unrelated to detachment tectonics, as proposed by Fournier et al. (2006). More likely, however, complying to crustal scale extension tectonic models as reviewed in Platt, Behr, and Cooper (2015) and Brun et al. (2018), the steep faulting in the upper-plate formed after abandonment of the rotated Banurama Detachment when a new detachment nucleated at deeper crustal levels (Figure 1). This is similar to descriptions from the Dolomites (Massari & Neri, 1997) and the Sacramento Basin (Fedo & Miller, 1992), and conforms to the observation of the Banurama Detachment below the Jafnayn Formation resting on ophiolite in the footwall of the Wadi Kabir Fault (Figure 4c). Nevertheless, the general northerly accommodation increase linked with the Banurama Detachment became modified by displacement on the Marina and Yiti Beach faults, giving a rift-style topography/bathymetry filled by carbonate growth packages organized in well-defined facies belts (Figure 11). At this stage, the basin was barren of siliciclastic input, suggesting that slopes in continental uplands were tilted away from the basin. This would be expected by footwall rebound behind normal faults (e.g. Gawthorpe & Leeder, 2000).

6 | MORPHOLOGY AND GEOGRAPHY DURING BASIN FORMATION

Sediments shed from the exhumed Saih Hatat culmination were deposited in evolving extensional basins in NE

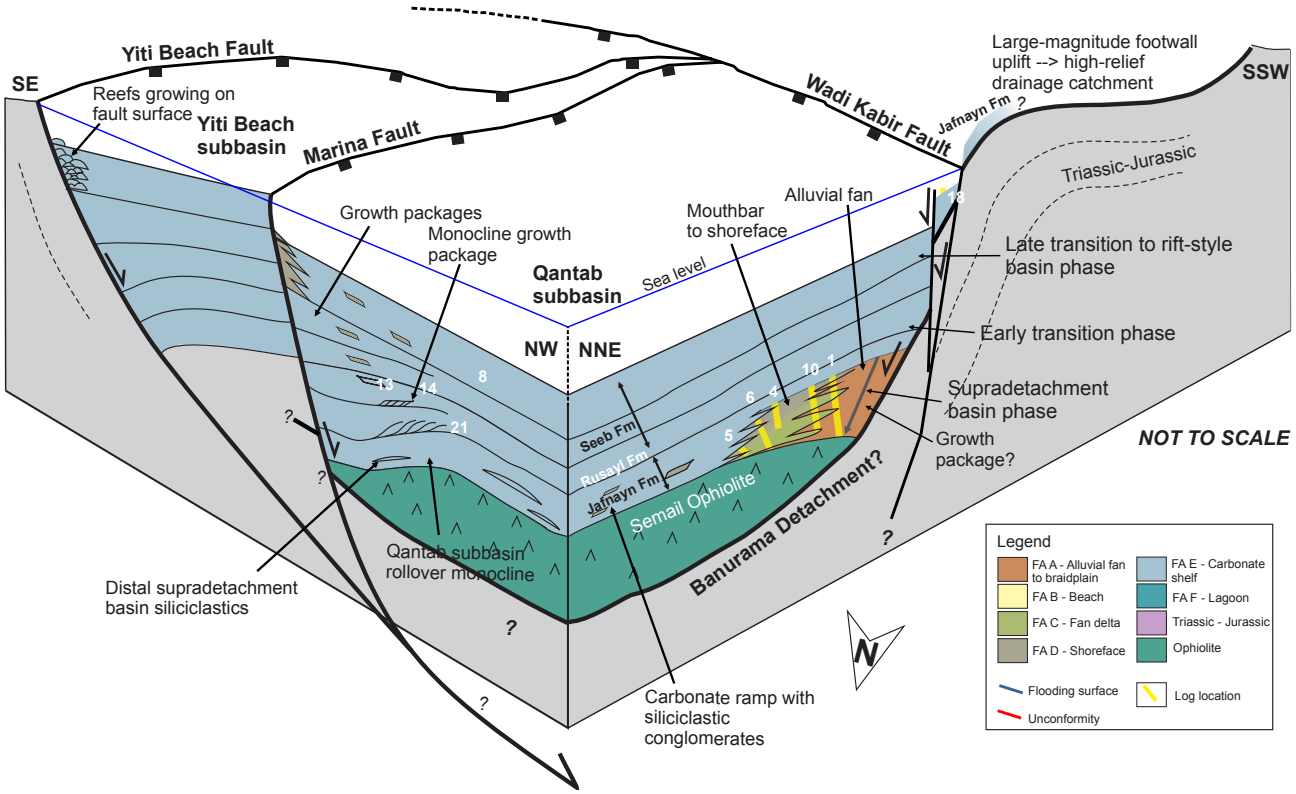

FIGURE 11 Schematic model of the Bandar Jissah Basin during deposition of the upper Seeb Formation. Accommodation was first controlled by the Banurama Detachment and later modified by steep faults

Oman from the Maastrichtian onward following collapse of the orogen that constituted the paleo-Oman Mountains (e.g. Abbasi et al., 2014; Braathen & Osmundsen, 2020). Significant siliciclastic input to these basins, indicating the topographic prominence of Saih Hatat, has been documented in the Late Cretaceous Al Khawd Formation, late Paleocene to early Eocene Jafnayn Formation and early to middle Eocene Rusayl Formation (Dill et al., 2007; Fournier et al., 2006; Mann et al., 1990; Nolan et al., 1990; Searle, 2007). It has been suggested that the Saih Hatat was submerged by middle Eocene times on the basis of lacking siliciclastic input and few evidence for subaerial exposure during deposition of the Seeb Formation (Hansman et al., 2017; Nolan et al., 1990). Stratigraphy in the Bandar Jissah Basin, however, records both a significant siliciclastic input and prolonged periods of subaerial exposure during deposition of the Seeb Formation (Figures 3 and 5 – logs 15 and 19; Supplementary Material). These observations suggest both active tectonics and presence of a sediment-producing hinterland during the middle Eocene. Our subdivision of the basin evolution into three phases (supradetachment basin, early transition and late transition to rift-style basin phase) reflect changes in basin configurations that impact sedimentary systems in the basin. Furthermore, the changing basin configuration alters the significance of uplands south of the study area as sediment sources. The early wave of coarse clastic sediments discharged into a shallow but broad marine basin became obstructed as the basin starts to roll over in a growth monocline, coinciding with regressive events that facilitate development of karst and paleosols. This potentially reflects the arrival of isostasy-driven uplift and deactivation of the Banurama Detachment. When significant accommodation again developed, clean carbonate growth sections were deposited proximal to steep normal faults in a configuration of fault blocks.

7 | FAULT CONTROL ON CURRENT OUTCROP PATTERN

The distribution of outcrops in ancient extensional basin systems may reflect characteristics of their controlling faults. In the hanging wall of the Wadi Kabir Fault, Paleogene sediments and the Semail Ophiolite outcrop, respectively, in synclines (Qantab and Al Bustan) and anticlines (area between Qantab and Al Bustan, Wadi al Kabir urban area) that are perpendicular to the fault. Such transverse structures are common in extensional basin systems (see e.g. Friedmann & Burbank, 1995; Schlische, 1995; Gawthorpe & Leeder, 2000; Kapp et al., 2008; Serck & Braathen, 2019). The transverse folds in the Bandar Jissah Basin and adjacent areas may be explained by both

detachment and rift tectonics; either reflecting corrugations in the underlying Banurama Detachment or resulting from fault displacement variations along an initially segmented Wadi Kabir Fault. The transverse fold axes, however, are both roughly parallel with the kinematic axis of the Banurama Detachment, and perpendicular to the strike of the Wadi Kabir Fault (Figure 2b). Moreover, because of limited along-strike exposure of the Banurama Detachment and few indications of initial segmentation of the Wadi Kabir Fault, such as breached relay structures, the origin of the transverse folds remain elusive. We note, however, that transverse folds contribute to controlling the present-day outcrop pattern, and that the Bandar Jissah Basin was likely much wider than in its current configuration as it evolved as a supradetachment basin in the hanging wall of the Banurama Detachment from the late Paleocene to early Eocene.

8 | CONCLUSIONS

This study documents the tectonostratigraphic development of the Paleogene Bandar Jissah Basin, which occupied a position between the Late Cretaceous obduction orogeny and the Tethys Ocean. The Bandar Jissah Basin resulted from different modes of extensional tectonics, and the basin fill records both substantial siliciclastic input from external catchment areas as well as extensive carbonate production within the basin. We establish how faulting and fault-related folding controlled accommodation development and facies distribution during basin history, as follows:

1. The stratigraphy and structures mapped in the Bandar Jissah Basin document a transition from continental to marine depositional environments influenced by active faulting. Changes in sedimentary style and distribution reflect a transition from a supradetachment basin setting to a rift-style basin setting through three phases;
2. *Supradetachment phase*: The Bandar Jissah Basin initiated as a supradetachment basin in the late Paleocene, when a siginificant pulse of continental conglomerates mixed with shallow marine carbonate ramp deposits of the late Paleocene to early Eocene Jafnayn Formation were deposited onto ophiolitic rocks above the Banurama Detachment.
3. *Early transition phase*: During deposition of the early to middle Eocene Rusayl Formation and lower part of the middle Eocene Seeb Formation, the overall northerly increase in accommodation was modified by growth of the Qantab subbasin monocline, which was caused by rollover into the Banurama Detachment. Decreasing siliciclastic input during this time, together with regressive events that result in karstification and paleosol development, signal a re-configuration of hinterland drainages that likely relates to isostasy-driven uplift and abandonment of the Banurama Detachment.
4. *Late transition to rift-style basin phase*: Fault-related sedimentary growth packages and alignment of facies belts to fault strike suggest the steep Marina, Yiti Beach and Wadi Kabir faults controlled accommodation during deposition of the upper section of the Eocene Seeb Formation. The Wadi Kabir Fault cut and offset the Banurama Detachment and supradetachment basin down towards the northeast.
5. The evolution of basin style suggested herein agrees with models deduced from other supradetachment basins, where isostatic uplift following large-magnitude faulting caused abandonment of detachment faults. Subsequent extension manifests as steep faults that dissect the upper plate, altering drainage patterns and accommodation distribution.
6. Paleogene basins around Muscat were likely much larger than reflected in the current outcrop pattern. Transverse folds that either represent corrugations on the Banurama Detachment or result from displacement variations along an initially segmented Wadi Kabir Fault have modified the hanging wall geometry and ultimately affected which parts of the Bandar Jissah Basin were preserved and eroded.

ACKNOWLEDGEMENTS

The first author, Snorre Olaussen, Ivar Midtkandal and Anna Elisabeth van Yperen thanks the LoCrA consortium (Lower Cretaceous basin studies in the Arctic) for financial support. Additionally the first author, Alvar Braathen, Per Terje Osmundsen, Snorre Olaussen and Ivar Midtkandal acknowledge backing from the Suprabasins project (Research Council of Norway grant no. 295208) and the Akademia program at the University of Oslo (sponsored by Equinor). Kjetil Indrevær thanks the ARCEx project (Research Centre for Arctic Petroleum Exploration) (Research Council of Norway grant no. 228107) for funding. We are grateful for Dr. Michelle McMahon's support in the field and to Professor Lars Stemmerik for fruitful discussions. Associate editor Craig Magee and reviewers Riccardo Asti and Andreas Scharf are sincerely thanked for their insightful and detailed feedback that helped improve the manuscript.

CONFLICT OF INTEREST

No conflict of interest declared.

DATA AVAILABILITY STATEMENT

The data that support the findings of this study are available from the corresponding author upon reasonable request.

ORCID

Christopher Sæbø Serck https://orcid.org/0000-0002-8829-0270
Alvar Braathen https://orcid.org/0000-0002-0869-249X
Ivar Midtkandal https://orcid.org/0000-0002-4507-288X

REFERENCES

Abbasi, I. A., Salad Hersi, O., & Al-Harthy, A. (2014). Late Cretaceous conglomerates of the Qahlah formation, north Oman. *Geological Society, London, Special Publications*, *392*(1), 325–341. https://doi.org/10.1144/SP392.17

Ali, M. Y., & Watts, A. B. (2009). Subsidence history, gravity anomalies and flexure of the United Arab Emirates (UAE) foreland basin. *GeoArabia*, *14*(2), 17–44.

Asti, R., Faccenna, C., Rossetti, F., Malusà, M. G., Gliozzi, E., Faranda, C., … Cosentino, D. (2019). The Gediz supradetachment system (SW Turkey): Magmatism, tectonics, and sedimentation during crustal extension. *Tectonics*, *38*(4), 1414–1440. https://doi.org/10.1029/2018TC005181

Asti, R., Malusà, M. G., & Faccenna, C. (2018). Supradetachment basin evolution unravelled by detrital apatite fission track analysis: The Gediz Graben (Menderes Massif, Western Turkey). *Basin Research*, *30*(3), 502–521. https://doi.org/10.1111/bre.12262

Beavington-Penney, S. J., Wright, V. P., & Racey, A. (2006). The Middle Eocene Seeb Formation of Oman: An investigation of acyclicity, stratigraphic completeness, and accumulation rates in shallow marine carbonate settings. *Journal of Sedimentary Research*, *76*(10), 1137–1161. https://doi.org/10.2110/jsr.2006.109

Bhattacharya, J. P. (2006). Deltas. In H. W. Posamentier, & R. G. Walker (Eds.), *Facies models revisited* (pp. 237–292). Tulsa, OK: SEPM Speci. SEPM Society for Sedimentary Geology. https://doi.org/10.2110/pec.06.84.0237

Braathen, A., Bælum, K., Maher, H. Jr, & Buckley, S. J. (2011). Growth of extensional faults and folds during deposition of an evaporite-dominated half-graben basin; the Carboniferous Billefjorden Trough, Svalbard. *Norsk Geologisk Tidsskrift*, *91*(3), 137–161.

Braathen, A., & Osmundsen, P. T. (2020). Extensional tectonics rooted in orogenic collapse: Long-lived disintegration of the Semail Ophiolite, Oman. *Geology*, *48*(3), 258–262. https://doi.org/10.1130/G47077.1

Braathen, A., Osmundsen, P. T., & Gabrielsen, R. H. (2004). Dynamic development of fault rocks in a crustal-scale detachment: An example from western Norway. *Tectonics*, *23*(4), 1–21. https://doi.org/10.1029/2003TC001558

Braathen, A., Osmundsen, P. T., Nordgulen, Ø., Roberts, D., & Meyer, G. B. (2002). Orogen-parallel extension of the Caledonides in northern central Norway: An Overview. *Norwegian Journal of Geology*, *82*, 225–241. https://doi.org/10.1130/0091-7613(2000)28

Brun, J.-P., Sokoutis, D., Tirel, C., Gueydan, F., Van Den Driessche, J., & Beslier, M.-O. (2018). Crustal versus mantle core complexes. *Tectonophysics*, *746*, 22–45. https://doi.org/10.1016/j.tecto.2017.09.017

Clifton, H. E. (2006). A reexamination of facies models for clastic shorelines. *SEPM Special Publications*, *84*, 293–338.

Clifton, H. E., Hunter, R. E., & Phillips, R. L. (1971). Depositional structures and processes in the non-barred high-energy nearshore. *Journal of Sedimentary Petrology*, *41*(3), 651–670. https://doi.org/10.1306/74D7231A-2B21-11D7-8648000102C1865D

Cooper, D. J. W., Ali, M. Y., & Searle, M. P. (2014). Structure of the northern Oman Mountains from the Semail Ophiolite to the Foreland Basin. *Geological Society, London, Special Publications*, *392*, 129–153. https://doi.org/10.1144/sp392.7

Cross, N. E., & Bosence, D. W. J. (2008). 'Tectono-sedimentary models for rift-basin carbonate systems'. *Controls on carbonate platform and reef development* (Vol. *89*, pp. 83–105). Tulsa, OK: SEPM Special Publication. https://doi.org/10.2110/pec.08.89.0083

Cross, N. E., Purser, B. H., & Bosence, D. J. W. (1998). 'The tectono-sedimentary evolution of a rift margin carbonate platform: Abu Shaar, Gulf of Suez, Egypt', in. In B. H. Purser, & D. J. W. Bosence (Eds.), *Sedimentation and tectonics in rift basins red sea:- gulf of Aden*. Dordrecht: Springer. https://doi.org/10.1007/978-94-011-4930-3_16

Denizot, M., & Massieux, M. (1965). Observations sur le genre Distichoplax (algues Mélobésiées). *Bulletin de la Societe Geologique de France*, *7*, 387–391.

Dietrich, W. O. (1927). Die geologisch-stratigraphischen Ergebnisse der Routenaufnahmen durch Ostpersien-Sven Hedin. *Eine Routenaufnahmen durch Ostpersien*, *2*, 447–464.

Dill, H. G., Wehner, H., Kus, J., Botz, R., Berner, Z., Stüben, D., & Al-Sayigh, A. (2007). The Eocene Rusayl Formation, Oman, carbonaceous rocks in calcareous shelf sediments: Environment of deposition, alteration and hydrocarbon potential. *International Journal of Coal Geology*, *72*(2), 89–123. https://doi.org/10.1016/j.coal.2006.12.012

Dorobek, S. L. (2008). Syn-rift carbonate platform sedimentation. *SEPM Special Publications*, *89*, 57–81.

Dunham, R. J. (1962). 'Classification of carbonate rocks according to depositional texture'. In W. E. Ham (Ed.). *Classification of carbonate rocks* (pp. 108–121). Tulsa, OK: American Association of Petroleum Geologists, Memoir 1.

Embry, A. F., & Klovan, J. E. (1971). A late Devonian reef tract on northeastern Banks Island, NWT. *Bulletin of Canadian Petroleum Geology*, *19*(4), 730–781.

Fedo, C. M., & Miller, J. M. G. (1992). Evolution of a Miocene half-graben basin, Colorado River extensional corridor, southeastern California. *Geological Society of America Bulletin*, *104*(4), 481–493. https://doi.org/10.1130/0016-7606(1992)104<0481:EOAMHG>2.3.CO;2

Fillmore, R. P., Walker, J. D., Bartley, J. M., & Glazner, A. F. (1994). Development of three genetically related basins associated with detachment-style faulting: Predicted characteristics and an example from the central Mojave Desert, California. *Geology*, *22*(12), 1087–1090. https://doi.org/10.1130/0091-7613(1994)022<1087:DOTGRB>2.3.CO;2

Fournier, M., Lepvrier, C., Razin, P., & Jolivet, L. (2006). Late Cretaceous to Paleogene post-obduction extension and subsequent Neogene compression in the Oman Mountains. *GeoArabia*, *11*(4), 17–40.

Friedman, G. M. (1988). Case histories of coexisting reefs and terrigenous sediments: The Gulf of Elat (Red Sea), Java Sea, and Neogene basin of the Negev, Israel. *Developments in Sedimentology*, *42*, 77–97.

Friedmann, S. J., & Burbank, D. W. (1995). Rift basins and supradetachment basin: Intracontinental extensional end members. *Basin Research*, *7*(2), 109–127. https://doi.org/10.1111/j.1365-2117.1995.tb00099.x

Gawthorpe, R. L., Fraser, A. J., & Collier, R. E. L. (1994). Sequence stratigraphy in active extensional basins: Implications for the

interpretation of ancient basin-fills. *Marine and Petroleum Geology*, *11*(6), 642–658. https://doi.org/10.1016/0264-8172(94)90021-3

Gawthorpe, R. L., & Leeder, M. R. (2000). Tectono-sedimentary evolution of active extensional basins. *Basin Research*, *12*(3–4), 195–218. https://doi.org/10.1111/j.1365-2117.2000.00121.x

Glennie, K. W., Boeuf, M. G. A., Hughes Clarke, M. W., Moody-Stuart, M., Pilaar, W. F. H., & Reinhardt, B. M. (1973). Late Cretaceous nappes in Oman Mountains and their geologic evolution. *AAPG Bulletin*, *57*(1), 5–27. Retrieved from http://archives.datapages.com/data/bulletns/1971-73/images/pg/00570001/0000/00050.pdf (Accessed: 22 November 2018).

Glennie, K. W., Boeuf, M. G. A., Hughes Clarke, M. W., Moody-Stuart, M., Pilaar, W. F. H., & Reinhardt, B. M. (1974). Geology of the Oman mountains. *Verhandelingen Koninklijk Nederlands Geologisch Mijnbouwkundidg Genootschap*, *31*, 423.

Gray, D. R., Kohn, B. P., Gregory, R. T., & Raza, A. (2006). Cenozoic exhumation history of the Oman margin of Arabia based on low-T thermochronology. *Geochimica et Cosmochimica Acta*, *70*(18), A213. https://doi.org/10.1016/j.gca.2006.06.428

Grohmann, C. H., & Campanha, G. A. (2010). OpenStereo: Open source, cross-platform software for structural geology analysis. In *AGU Fall Meeting Abstracts*.

Gupta, S., Cowie, P. A., Dawers, N. H., & Underhill, J. R. (1998). A mechanism to explain rift-basin subsidence and stratigraphic patterns through fault-array evolution. *Geology*, *26*(7), 595–598. https://doi.org/10.1130/0091-7613(1998)026<0595:AMTERB>2.3.CO;2

Hansman, R. J., Ring, U., Thomson, S. N., den Brok, B., & Stübner, K. (2017). Late Eocene Uplift of the Al Hajar Mountains, Oman, supported by stratigraphy and low-temperature thermochronology. *Tectonics*, *36*(12), 3081–3109. https://doi.org/10.1002/2017TC004672

Haynes, J. R., Racey, A., & Whittaker, J. E. (2010). 'A revision of the Early Palaeogene nummulitids (Foraminifera) from northern Oman, with implications for their classification'. In J. E. Whittaker & M. B. Hart (Eds.), *Micropaleontology, Sedimentary environments and Stratigraphy* (pp. 29–89). London: Geological Society of London. The Microp. https://doi.org/10.1144/TMS004.4

Henstra, G. A., Gawthorpe, R. L., Helland-Hansen, W., Ravnås, R., & Rotevatn, A. (2017). Depositional systems in multiphase rifts: Seismic case study from the Lofoten margin, Norway. *Basin Research*, *29*(4), 447–469. https://doi.org/10.1111/bre.12183

Holmes, A. E., & Christie-Blick, N. (1993). 'Origin of sedimentary cycles in mixed carbonate-Siliciclastic systems: An example from the Canning Basin, Western Australia: Chapter 7', *AAPG Memoirs*, 57 (pp. 181–212).

Jolivet, L., Goffé, B., Bousquet, R., Oberhänsli, R., & Michard, A. (1998). Detachments in high-pressure mountain belts, Tethyan examples. *Earth and Planetary Science Letters*, *160*(1–2), 31–47. https://doi.org/10.1016/S0012-821X(98)00079-X

Kapp, P., Taylor, M., Stockli, D., & Ding, L. (2008). Development of active low-angle normal fault systems during orogenic collapse: Insight from Tibet. *Geology*, *36*(1), 7–10. https://doi.org/10.1130/G24054A.1

Le Métour, J., Béchennec, F., Roger, J., & Wyns, R. (1992). *Geological map of Muscat, with explanatory notes, sheet NF 40–04, scale 1: 250,000*. Sultanate of Oman: Ministry of Petroleum and Minerals, Directorate General of Minerals.

Lippard, S. J. (1983). Cretaceous high pressure metamorphism in NE Oman and its relationship to subducted and ophiolite nappe emplacement. *Journal of the Geological Society*, *140*(1), 97–104. https://doi.org/10.1144/gsjgs.140.1.0097

Lippard, S. J., Shelton, A. W., & Gass, I. G. (1986). The ophiolite of northern Oman. *Geological Society, London, Memoirs*, *11*, 178. Published for the Geological Society by Blackwell Scientific Publications. Retrieved from https://books.google.no/books/about/The_Ophiolite_of_Northern_Oman.html?id=PCkcAQAAIAAJ&redir_esc=y (Accessed 22 November, 2018).

Lister, G. S., & Davis, G. A. (1989). The origin of metamorphic core complexes and detaehment faults formed during Tertiary eontinental margins. *Geology*, *14*(1), 246–250. Retrieved from http://d.wanfangdata.com.cn/NSTLQK_10.1130-0091-7613(1986)14-246-DFATEO-2.0.CO%5Cn2.aspx%5Cnpapers3://publication/uuid/F517183C-D20A-4974-A72B-6868A7557C69

Manatschal, G. (2004). New models for evolution of magma-poor rifted margins based on a review of data and concepts from West Iberia and the Alps. *International Journal of Earth Sciences*, *93*(3), 432–466. https://doi.org/10.1007/s00531-004-0394-7

Mann, A., Hanna, S. S., Nolan, S. C., Mann, A., & Hanna, S. S. (1990). The post-Campanian tectonic evolution of the central Oman Mountains: Tertiary extension of the eastern Arabian Margin. *The Geology and Tectonics of the Oman Region*, *49*(1), 549–563. https://doi.org/10.1144/gsl.sp.1992.049.01.33

Massari, F., & Neri, C. (1997). Sedimentary geology the infill of a supradetachment (?) basin: The continental to shallow-marine Upper Permian succession in the Dolomites and Carnia (Italy). *Sedimentary Geology*, *110*, 181–221. https://doi.org/10.1016/S0037-0738(96)00084-X

Mattern, F., & Bernecker, M. (2018). A shallow marine clinoform system in limestones (Paleocene/Eocene Jafnayn Formation, Oman): Geometry, microfacies, environment and processes. *Carbonates and Evaporites*, *34*(1), 101–113. https://doi.org/10.1007/s13146-018-0444-z

Mattern, F., & Scharf, A. (2018). Postobductional extension along and within the Frontal Range of the eastern Oman Mountains. *Journal of Asian Earth Sciences*, *154*, 369–385. https://doi.org/10.1016/j.jseaes.2017.12.031

Mount, V. S., Crawford, R. I. S., & Bergman, S. C. (1998). Regional structural style of the central and southern Oman Mountains: Jebel Akhdar, Saih Hatat, and the northern Ghaba Basin. *GeoArabia*, *3*(4), 475–490.

Nolan, S. C., Skelton, P. W., Clissold, B. P., & Smewing, J. D. (1990). Maastrichian to early tertiary stratigraphy and paleogeography of the central and northern Oman Mountains. *The Geology and Tectonics of the Oman Region*, *49*(49), 495–512. https://doi.org/10.1144/GSL.SP.1992.049.01.31

Oner, Z., & Dilek, Y. (2011). Supradetachment basin evolution during continental extension: The Aegean province of western Anatolia, Turkey. *GSA Bulletin*, *123*(11), 2115–2141. https://doi.org/10.1130/B30468.1

Osmundsen, P. T., & Andersen, T. B. (2001). The middle Devonian basins of western Norway: Sedimentary response to large-scale transtensional tectonics? *Tectonophysics*, *332*(1–2), 51–68. https://doi.org/10.1016/S0040-1951(00)00249-3

Osmundsen, P. T., Bakke, B., Svendby, A. K., & Andersen, T. B. (2000). Architecture of the Middle Devonian Kvamshesten Group, western Norway: Sedimentary response to deformation above a ramp-flat extensional fault. *Geological Society, London, Special Publications*, *180*(1), 503–535. https://doi.org/10.1144/gsl.sp.2000.180.01.27

Osmundsen, P. T., & Péron-Pinvidic, G. (2018). Crustal-scale fault interaction at rifted margins and the formation of domain-bounding breakaway complexes: Insights from offshore Norway. *Tectonics*, *37*(3), 935–964. https://doi.org/10.1002/2017TC004792

Özcan, E., Abbasi, İ. A., Drobne, K., Govindan, A., Jovane, L., & Boukhalfa, K. (2016). Early Eocene orthophragminids and alveolinids from the Jafnayn Formation, N Oman: Significance of *Nemkovella stockari Less* & Özcan, 2007 in Tethys. *Geodinamica Acta*, *28*(3), 160–184. https://doi.org/10.1080/09853111.2015.1107437

Paerl, H. W., Pinckney, J. L., & Steppe, T. F. (2000). Cyanobacterial-bacterial mat consortia: Examining the functional unit of microbial survival and growth in extreme environments. *Environmental Microbiology*, *2*(1), 11–26. https://doi.org/10.1046/j.1462-2920.2000.00071.x

Patruno, S., Hampson, G. J., & Jackson, C. A. L. (2015). Quantitative characterisation of deltaic and subaqueous clinoforms. *Earth-Science Reviews*, *142*, 79–119. https://doi.org/10.1016/j.earscirev.2015.01.004

Pia, J. (1934). Kalkalgen aus dem Eozän der Felsen von Hrièovské Podhradie in Waagtal. *Véstnik du Service Géologique de la République Tchécoslovaque*, *10*, 14–18.

Platt, J. P., Behr, W. M., & Cooper, F. J. (2015). Metamorphic core complexes: Windows into the mechanics and rheology of the crust. *Journal of the Geological Society*, *172*(1), 9–27. https://doi.org/10.1144/jgs2014-036

Racey, A. (1995). Lithostratigraphy and larger foraminiferal (nummulitid) biostratigraphy of the tertiary of northern Oman. *Micropaleontology*, *41*, 1–123. https://doi.org/10.2307/1485849

Rattey, R. P., & Hayward, A. B. (1993). Sequence stratigraphy of a failed rift system: The Middle Jurassic to Early Cretaceous basin evolution of the Central and Northern North Sea. *Geological Society, London, Petroleum Geology Conference Series*, *4*(1), 215–249. https://doi.org/10.1144/0040215

Ravnås, R., & Steel, R. J. (1998). Architecture of marine rift basin successions. *AAPG Bulletin*, *82*(1), 110–146. https://doi.org/10.1306/1D9BC3A9-172D-11D7-8645000102C1865D

Ricateau, R., & Riche, P. H. (1980). Geology of the Musandam peninsula (Sultanate of Oman) and its surroundings. *Journal of Petroleum Geology*, *3*(2), 139–152. https://doi.org/10.1306/BF9AB5C2-0EB6-11D7-8643000102C1865D

Roberts, H. H., & Murray, S. P. (1988). Gulfs of the Northern Red Sea: Depositional settings of abrupt siliciclastic-carbonate transitions. *Developments in Sedimentology*, *42*, 99–142. https://doi.org/10.1016/S0070-4571(08)70166-3

Rollinson, H. R., Searle, M. P., Abbasi, I. A., Al-Lazki, A. I., & Al Kindi, M. H. (2014). Tectonic evolution of the Oman Mountains: An introduction. *Geological Society, London, Special Publications*, *392*(1), 1–7. https://doi.org/10.1144/SP392.1

Saddiqi, O., Michard, A., Goffe, B., Poupeau, G., & Oberhänsli, R. (2006). Fission-track thermochronology of the Oman Mountains continental windows, and current problems of tectonic interpretation. *Bulletin de la Société Géologique de France*, *177*(3), 127–134. https://doi.org/10.2113/gssgfbull.177.3.127

Schlische, R. W. (1995). Geometry and origin of fault-related folds in extensional settings. *AAPG Bulletin*, *79*(11), 1661–1678. https://doi.org/10.1306/7834DE4A-1721-11D7-8645000102C1865D

Searle, M. P. (2007). Structural geometry, style and timing of deformation in the Hawasina Window, Al Jabal al Akhdar and Saih Hatat culminations, Oman Mountains. *GeoArabia*, *12*(2), 99–130.

Searle, M. P., & Ali, M. Y. (2009). Structural and tectonic evolution of the Jabal Sumeini – Al Ain – Buraimi region, northern Oman and eastern United Arab Emirates. *GeoArabia*, *14*(1), 115–142.

Searle, M. P., Warren, C. J., Waters, D. J., & Parrish, R. R. (2004). Structural evolution, metamorphism and restoration of the Arabian continental margin, Saih Hatat region, Oman Mountains. *Journal of Structural Geology*, *26*(3), 451–473. https://doi.org/10.1016/j.jsg.2003.08.005

Serck, C. S., & Braathen, A. (2019). Extensional fault and fold growth: Impact on accommodation evolution and sedimentary infill. *Basin Research*, *31*(5), 967–990. https://doi.org/10.1111/bre.12353

Sharp, I. R., Gawthorpe, R. L., Underhill, J. R., & Gupta, S. (2000). Fault-propagation folding in extensional settings: Examples of structural style and synrift sedimentary response from the Suez rift, Sinai, Egypt. *Bulletin of the Geological Society of America*, *112*(12), 1877–1899. https://doi.org/10.1130/0016-7606(2000)112<1877:F-PFIES>2.0.CO;2

Smyrak-Sikora, A., Johannessen, E. P., Olaussen, S., Sandal, G., & Braathen, A. (2019). Sedimentary architecture during carboniferous rift initiation – The arid Billefjorden Trough, Svalbard. *Journal of the Geological Society*, *176*(2), 225–252. https://doi.org/10.1144/jgs2018-100

Spalletti, L. A., Franzese, J. R., Matheos, S. D., & Schwarz, E. (2000). Sequence stratigraphy of a tidally dominated carbonate–siliciclastic ramp; the Tithonian-Early Berriasian of the Southern Neuquén Basin, Argentina. *Journal of the Geological Society*, *157*(2), 433–446. https://doi.org/10.1144/jgs.157.2.433

Stein, R. S., & Barrientos, S. E. (1985). Planar high-angle faulting in the Basin and Range: Geodetic analysis of the 1983 Borah Peak, Idaho, Earthquake. *Journal of Geophysical Research*, *90*(B13), 355–366. https://doi.org/10.1029/JB090iB13p11355

Sutra, E., Manatschal, G., Mohn, G., & Unternehr, P. (2013). Quantification and restoration of extensional deformation along the Western Iberia and Newfoundland rifted margins. *Geochemistry, Geophysics, Geosystems*, *14*(8), 2575–2597. https://doi.org/10.1002/ggge.20135

Talling, P. J., Masson, D. G., Sumner, E. J., & Malgesini, G. (2012). Subaqueous sediment density flows: Depositional processes and deposit types. *Sedimentology*, *59*(7), 1937–2003. https://doi.org/10.1111/j.1365-3091.2012.01353.x

Thrana, C., & Talbot, M. R. (2006). High-frequency carbonate-siliciclastic cycles in the Miocene of the Lorca Basin (Western Mediterranean, SE Spain). *Geologica Acta*, *4*(3), 343–354. https://doi.org/10.1344/105.000000348

van Hinsbergen, D. J. J., & Meulenkamp, J. E. (2006). Neogene supradetachment basin development on Crete (Greece) during exhumation of the South Aegean core complex. *Basin Research*, *18*(1), 103–124. https://doi.org/10.1111/j.1365-2117.2005.00282.x

Vetti, V. V., & Fossen, H. (2012). Origin of contrasting Devonian supradetachment basin types in the Scandinavian Caledonides. *Geology*, *40*(6), 571–574. https://doi.org/10.1130/G32512.1

Warren, C. J., & Miller, J. M. L. (2007). Structural and stratigraphic controls on the origin and tectonic history of a subducted continental margin, Oman. *Journal of Structural Geology*, *29*(3), 541–558. https://doi.org/10.1016/j.jsg.2006.10.006

Wessels, R. J. F. (2012). *Post-obduction evolution of the Wadi Kabir syncline area and northern Saih Hatat, Oman*, Msc Thesis. Utrecht University.

White, R. S., & Ross, D. A. (1979). Tectonics of the western Gulf of Oman. *Journal of Geophysical Research*, *84*(B7), 3479–3489. https://doi.org/10.1029/JB084iB07p03479

Würsten, F., Flisch, M., Michalski, I., Le Métour, J., Mercolli, I., Matthäus, U., & Peters, T. (1991). The uplift history of the Precambrian crystalline basement of the Jabal J'alan (Sur Area). *Ophiolite Genesis and Evolution of the Oceanic Lithosphere*, *5*(1989), 613–626.

Zavala, C., Arcuri, M., Di Meglio, M., Diaz, H. G., & Contreras, C. (2011). A genetic facies tract for the analysis of sustained hyperpycnal flow deposits. *AAPG Special Volumes*, 31–51. https://doi.org/10.1306/13271349St613438

How to cite this article: Serck CS, Braathen A, Olaussen S, et al. Supradetachment to rift basin transition recorded in continental to marine deposition; Paleogene Bandar Jissah Basin, NE Oman. *Basin Res*. 2020;00:1–26. https://doi.org/10.1111/bre.12484